D4.2 Mobility models description

Deliverable ID:	D4.2
Dissemination Level:	PU
Project Acronym:	Modus
Grant:	891166
Call:	H2020-SESAR-2019-2
	SESAR-ERA-10-2019
Topic:	ATM Role in Intermodal Transport
Consortium Coordinator:	BHL
Edition date:	19 December 2022
Edition:	00.01.20
Template Edition:	02.00.05

Co-funded by
the European Union

Authoring & Approval

Authors of the document

Name / Beneficiary	Position / Title	Date
Elham Zareian / UoW	Consortium member	25 November 2022
Luis Delgado / UoW	Consortium member	25 November 2022
Andrew Cook / UoW	Consortium member	25 November 2022
Ernesto Gregori / INX	Consortium member	25 November 2022
Tatjana Bolić / UoW	Consortium member	25 November 2022
Hamid Kadour / ECTL	Consortium member	25 November 2022
Antonio Correas / SKY	Consortium member	25 November 2022
Annika Paul / BHL	Project coordinator	25 November 2022

Reviewers internal to the project

Name / Beneficiary	Position / Title	Date
Graham Tanner / UoW	Consortium member	07 December 2022
Annika Paul / BHL	Project coordinator	07 December 2022
Hamid Kadour / ECTL	Consortium member	07 December 2022

Reviewers external to the project

Name / Beneficiary	Position / Title	Date
N/A		

Approved for submission to the SJU By - Representatives of beneficiaries involved in the project

Name / Beneficiary	Position / Title	Date
Annika Paul / BHL	Project coordinator	19 December 2022

Rejected By - Representatives of beneficiaries involved in the project

Name and/or Beneficiary	Position / Title	Date
N/A		

Document History

Edition	Date	Status	Name / Beneficiary	Justification
00.01.00	28/10/2022	Release	Modus Consortium	New document for review by the SJU
00.01.10	08/12/2022	Revised version submitted	Modus consortium	Revised document submitted to the SJU

EUROPEAN PARTNERSHIP

Co-funded by the European Union

00.01.20	19/12/2022	Revised version submitted	Modus consortium	Revised document submitted to the SJU

Copyright Statement

Modus

MODELLING AND ASSESSING THE ROLE OF AIR TRANSPORT IN AN INTEGRATED, INTERMODAL TRANSPORT SYSTEM

Abstract

Air-rail multimodal mobility has the potential to play a significant role in addressing European mobility challenges such as emissions reduction goals, and capacity shortages, and in moving towards a wider European multimodal transport network. There is still a need to better understand the potential role of rail when substituting current air links both from a strategic and a full, tactical mobility perspective, particularly when passenger connections are considered. Here we present the development of an innovative approach towards data driven, integrated air-rail modelling, considering passenger door-to-door itineraries.

EUROPEAN PARTNERSHIP

Co-funded by the European Union

Table of Contents

EUROPEAN PARTNERSHIP

Co-funded by
the European Union

List of Tables

EUROPEAN PARTNERSHIP

Co-funded by
the European Union

List of Figures

EUROPEAN PARTNERSHIP

Co-funded by
the European Union

1 Introduction

This document sets out the main elements of two models used by Modus: the Mercury passenger mobility model and the EUROCONTROL R-NEST tool. Whilst these models will be run separately, with results reported in D5.2 (Final Project Results Report), underpinning commonalities to support the inclusion of a rail layer in both models, and for each to model the full door-to-door context of passenger multimodal journeys, are presented.

In some of the Modus scenarios to be presented in this document, journeys originally planned by air will be modelled in terms of the ability of the rail network to accommodate them, or legs thereof, for example during bans on short-haul flights. The substitution potential of air and rail applying modal choice analysis has been the subject of various studies. Travel time and frequency are some of the most important factors in terms of modal travel behaviour ([2], [3]), as are the fares. The analysis of 4815 routes in Spain, France and Germany revealed that for a 1% increase in the average level of fares, the average demand decreases by 5.34% in France, 9.11% in Germany and 10.78% in Spain [3].

A first network analysis was carried out in Modus to assess the maximum potential air replacement that can be achieved with the fast rail network in Europe. Figure 1 below presents the flights with a distance lower or equal to 1100 km (blue lines) operating in Europe with an overlap of the rail network (green lines), which could potentially be used to replace them. One of the challenges of replacing flights by rail is the impact of these replacements in passenger connectivity at hubs. Therefore, in this analysis data from a busy day in 2014 schedules and passenger itineraries are considered as modelled in the previous H2020-SESAR research project Domino [4]. Rail alternatives are extracted considering 2019 routes from the MERITS database [5].

Figure 1: Rail and air network considered

EUROPEAN PARTNERSHIP

Co-funded by the European Union

The analysis conducted assesses the impact of a flight ban, where a rail alternative is possible. Figure 2 presents the results obtained with the network previously described as a function of the length of the flight ban up to 1200 km.
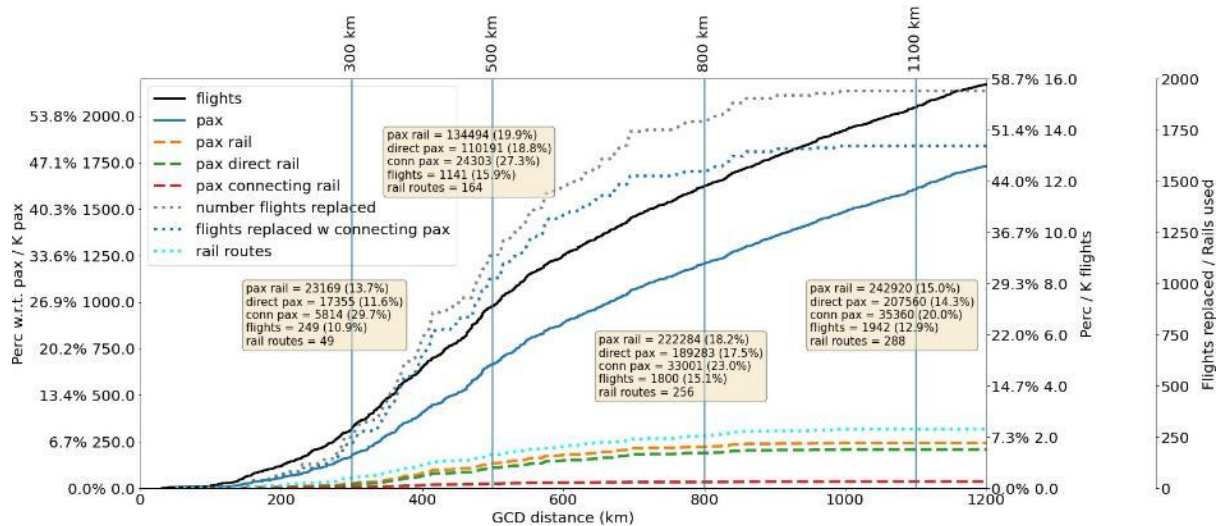

Figure 2: Impact of air-rail substitution for distances up to 1200 km

Figure 2 shows that flights up to about 1200 km account for almost 60% of flights considered in the analysis (right-hand y-axis). ≈1200 km represent almost 60% of all the schedules considered (almost 16 000 flights). From these, if the ban were to be introduced, fewer than 2000 flights would be affected, i.e. around 12% of flights. As shown in the figure, a ban of flights up to 1100 km would impact 1942 flights (12.9% of the flights considered in the analysis). The light blue dotes line shows that 288 rail routes are available for these origin-destination connections, i.e. flights on those connections can be replaced by rail. This would represent the use of 288 rail routes (origin-destinations connections by rail). It is interesting to observe how, as the ban distance increases, the number of flights impacted increases too, but from around 800 km the marginal gain diminishes significantly. At 800 km, 15.1% of the flights can be replaced (1800 flights) using already 256 rail routes (only 32 fewer rail routes than with a 1100km ban).

An interesting addition to the analysis is the consideration of passenger itineraries, including their flight connections at hubs. As shown in Figure 2Figure 2, the number of connecting passengers with respect to non-connecting ones that are replaced by rail as a function of distance decreases (from 29.7% of the passengers at 300 km, to 20% at 1100 km). However, even if the total number of connecting passengers is low, they have a significant impact on the number of flights which have at least a connecting passenger on them and that is replaced by rail. For example, at about 800 km a total of 1800 flights can be replaced by rail, but from these more than 1500 have some passengers with flight connections.

Policies such as the flight ban introduced in France might have very limited impact if limited to flights without connections, as short flights tend to include many feeders to the hub with connecting passengers. Connecting passengers are therefore not too significant in volume (around 20-25% of passengers being potentially moved to rail), but present a significant challenge for the replacement of air by rail. Multimodal itineraries are therefore a must when these substitution policies are considered.

Having set the scene for rail substitution and multimodality, we next turn to presenting the underpinning model components for Modus.

2 Model components

As already mentioned, passenger mobility will be assessed using two simulation models. Both models (Mercury, R-NEST) originated as air traffic simulators, and are being extended to take into account the possibility of rail travel and other components of the trips that are needed to calculate door-to-door metrics. The models encompass different trip stages, which differ slightly between air and rail parts. The modelling approach is the decomposition of the total travel into different stages.

The following tables summarise the stages of travel for passengers travelling by air, by rail and by both (i.e. multimodal journeys). For multimodal journeys (Table 3), four processes need to be considered, depending on access to the railway station.

Table 1: Travel stages of air passengers

Travel stage	Description
Door-to-kerb (D2K)	The time necessary to get from the home location to the entrance of the airport
Kerb-to-gate (K2G)	The time necessary to go through all the departure airport processes (luggage drop, security...) and reach the gate
Gate-to-gate (G2G)	The time necessary for the flight to arrive to the destination
Gate-to-kerb (G2K)	The time necessary to go through all the arrival airport processes (baggage claim, security...) and reach the entrance
Kerb-to-door (K2D)	The time necessary to get from the entrance of the airport to the final location

Table 2: Travel stages of rail passengers

Travel stage	Description
Door-to-platform (D2P)	The time necessary to get from the home location to the railway station platform
Platform-to-platform (P2P)	The time necessary for the train to arrive to the destination
Platform-to-door (P2D)	The time necessary to get from the railway station platform to the final location

EUROPEAN PARTNERSHIP

Co-funded by
the European Union

Table 3: Travel stages for multimodal journeys

Travel stage	Description
Gate-to-platform (G2P)	If railway station is located at the airport and onward segment of trip is by rail
Platform-to-gate (P2G)	If railway station is located at airport and prior flight segment of trip is by rail
Kerb-to-platform (K2P)	If railway station is not at the airport, e.g. at city centre, and onward segment of trip is by rail
Platform-to-kerb (P2K)	If railway station is not at the airport, e.g. at city centre, and prior flight segment of trip is by air

Therefore, a multimodal journey is possible if, for example, a passenger takes a plane and then a train from the city centre to get to their destination. The journey could comprise: door-to-kerb, kerb-to-gate, gate-to-gate, gate-to-platform, platform-to-platform and then platform-to-door.

The following sections address the development of city archetypes, first/last miles and airport processes.

2.1 City archetypes

2.1.1 Mapping 200 European airports to their corresponding NUTS3 regions

The modal choice model in WP3 was designed around the nomenclature of territorial units for statistics (NUTS) system at level 3 as the socio-economic parameters needed were available at that geographic granularity. The parameters included gross domestic product (GDP), unemployment rate, population by age group and gender, population by level of education achieved by gender and age, household income, level of rail infrastructure and international passenger transport. Therefore, it was important to map the airports to corresponding NUTS3 regions rather than assigning them to different cities. By assigning the airports to NUTS3 regions the distinctions between multiple airports within one city is easier. For example, London, has five airports, i.e. Heathrow, City, Gatwick, Luton, and Stansted. If we consider the origin-destination (OD) pair based on the city, it can include all the five airports. However, if the OD pair is considered based on the NUTS3 coding then it is clear which airport is specifically targeted. Therefore, as a result of mapping airports to the NUTS3 regions in the case of London there are exactly 5 NUTS 3 regions corresponding to the five airports. This task follows the steps below:

- Download NUTS3 regions coordinates from (https://ec.europa.eu/eurostat/web/gisco/geodata/reference-data/administrative-units-statistical-units/nuts);
- Extract level 3 coordinates from the main NUTS coordinates file;
- Having the coordinates of NUTS3 regions can help us considering each region as a polygon. Therefore, by developing an approach and having the coordinates of the 200 airports, for each airport we can identify which NUTS3 region it belongs to. It is worth mentioning that

some NUTS3 regions have more than one airport. e.g. Bromma Stockholm airport and Stockholm Arlanda airport are both identified by the same NUTS 3 coding;

- The final result of this mapping provides not only the NUTS3 code for each airport but also can identify each airport is located at which city.

2.1.2 Assignments of 200 airports (classified by NUTS3 codes) to appropriate city archetype levels

The holistic approach in Modus, integrating air and rail in the wider, door-to-door context, prompted the development of city archetypes, rather than focusing on airports or railway stations *per se*. A city archetype denotes a specific combination of airport and railway connections and allowed us to generalise the modelling based on the construction of typical urban travel infrastructure. This impacts the modelling at two levels. Firstly, it allows, holistically, the consideration of movements between 'Paris' and 'London' and the future of such flows, rather than being tied to specific constraints at particular airports, for example. Secondly, it allows the construction of urban mobility models relating, for example, to airport and railway station access and egress, with generic travel time distributions per archetype, drawing both on models of public transport data and a previous framework developed in the DATASET2050 project ([7], [9]). Table 4 summarises the main principles in defining five city archetype levels based on airport and railway station characteristics. In total, 200 European airports underpin the framework.

Table 4: Classification of city archetypes

City archetype	Airport archetype	Railway connection to airport	Further railway info (where applicable)
Arch-1	Main hub	Good inter-regional, direct HSR to airport	-
Arch-2	Main hub	Good inter-regional, no direct HSR to airport	HSR connected to the city only
Arch-3	Secondary hub	Good inter-regional, no direct HSR to airport	HSR connected to the region only and/or good mainline rail
Arch-4	Large/Medium	Good interregional, no direct HSR to airport	
Arch-5	National/regional	Near good inter-regional, no HSR	

2.1.3 Accounting for HSR in Europe

Identifying routes with *existing* HSR and *future* construction planning of such services, is one of the main principles in assigning an appropriate archetype level to a particular city. Furthermore, existing HSR services in Europe as well as any future construction planning helps to aid with the recovery under disruptions and other modelled scenarios such as, scenario 2 which represents the short-haul ban. The routes which already have HSRs running and the ones with construction planning in place (HSR ready to run by 2040) are identified and listed in Appendix A.

EUROPEAN PARTNERSHIP

Co-funded by the European Union

Therefore, implementing different scenarios (disruption scenarios and scenario 2), the air traffic flows on the identified routes are shifted to rail which results in quicker recovery on the affected routes. Figure 3 illustrates the routes with existing, under constructions and planned HSR services in Spain and Portugal.

Figure 3: High-speed lines in Portugal and Spain

(Source: UIC, Atlas: High-Speed Rail 2022)
(https://uic.org/passenger/highspeed/article/high-speed-data-and-atlas)

2.1.4 City-rail archetypes

As listed in the introductory part of this section (Table 2), the trips passengers take by rail are composed of the following stages: door-to-platform (D2P), platform-to-platform (P2P) and platform-to-door (P2D). In order to calculate the probabilistic distributions that describe the travel time in these stages, city-rail archetypes are included (as described in Table 5). The distributions themselves are further described later (Table 8).

Table 5: City-rail archetypes

EUROPEAN PARTNERSHIP

Co-funded by
the European Union

City-rail archetype	Categorisation
Large	> 1 million population
Medium	< 1 million population

2.2 First and last miles (door-to-kerb/door-to-platform) modelling

2.2.1 First and last miles context

Here, the objective is to compute the time taken during the first and last stages of the journey. In the cases where the first leg of the journey corresponds to a flight, this stage covers travel from the original departure point to the airport. The door-to-kerb time is based on the connections from the home location to the airport. If passengers use rail as an alternative to flights, then the first stage of the journey would involve travelling to the train station instead of the airport, hence the door-to-kerb model is replaced with the door-to-platform model. For Modus, the times to get from a specific point to the airport and from the airport to the same point are supposed to be equivalent in the probabilistic sense. Therefore, the same model can be used to compute the kerb-to-door times, that correspond to the final part of the journey once the passenger has arrived to their destination and have to get to a specific point of the arrival city. The same logic is applied to the door-to-platform and platform-to-door times. The following sub-sections describe the generation of travel time statistical distributions for door-to-kerb (and kerb-to-door) and door-to-platform (and platform-to-door).

2.2.2 Synthetic data on city archetypes for the door-to-kerb model

Cities are spaces containing hubs of more than one transportation mode. Models developed in WP4 account for long-distance air and rail travel between European cities. In addition, to have a complete view of the end-to-end journey, it is necessary to also account for passenger connectivity within the city, both as last-mile (airport or railway station to home/office, home/office to airport or railway station) and intermodal changes (airport-rail, rail-airport). The time taken when changing transport modes gives information of the frictions created at the local level, and allows us to compare performance of modal choices. Synthetic datasets have been generated using Skymantics routing engine (http://skymantics.com/geospatial-services/) to simulate the fastest/shortest routes between airports/railway stations and other locations in an urban environment. These locations include any other point in the city and surrounding region that is relevant as an origin or destination of travel, i.e. catchment area, defined concentrically around city airports or railway stations. The resulting datasets represent the catchment areas in terms of required travel time, for different configurations (i.e., airport archetypes and access mode).

2.2.3 City archetypes mobility modelling approach

The passenger mobility modelling requires a model of the door-to-door travel times based on the pair of city/archetypes involved. To include intermodal exchanges within the travel chain, the following approach has been followed.

EUROPEAN PARTNERSHIP

Co-funded by the European Union

2.2.3.1 Selection of city/airport examples which represent the airside archetypes

The following cities and airports have been selected due to availability of data and representativity of archetypes. Some of the cities contain more than one airport in the area, which allows us to calculate travel times reusing the same city transportation model, thus raising the efficiency of the generation effort.

Table 6: Example cities and airports illustrating the five city archetypes

City	Airport name (IATA, ICAO codes)	Archetype
Paris	Paris Charles de Gaulle airport (CDG, LFPG)	Arch-1 (main hub, HSR station at the airport, integrated in city/region transport network)
	Paris Orly airport (ORY, LFPO)	Arch-2 (main hub, HSR station in the city, integrated in city/region transport network)
	Paris Beauvais airport (BVA, LFOB)	Arch-5 (national/regional, no HSR station in the city, very loosely integrated in city/region transport network by shuttle to Paris)
Madrid	Adolfo Suárez Madrid-Barajas airport (MAD, LEMD)	Arch-2 (main hub, HSR station in the city, integrated in city/region transport network)
Stockholm	Stockholm Arlanda airport (ARN, ESSA)	Arch-3 (secondary hub, no HSR station in the city, loosely integrated in city/region transport network by shuttle and express train)
Brussels	Brussels airport (BRU, EBBR)	Arch-2 (main hub, HSR station in the city, integrated in city/region transport network)
	Brussels South Charleroi airport (CRL, EBCI)	Arch-4 (secondary hub, no HSR station in the city, loosely integrated in city/region transport network by shuttle to neighbouring cities)

2.2.3.2 Calculation of fastest-travel time catchment areas of airports and railway stations located in the selected examples

The dataset for Modus has been generated to represent the catchment area to the city airport/railway station of choice based on fastest travel time metrics. For cities with multiple airports, catchment areas are generated for each airport separately. The extension of the area calculation for each city was selected to cover all the airports as well as the whole metropolitan area. Per airport, two separate catchment area layers are generated representing different modal choices and making use of different datasets:

- Private vehicle (including taxi or ride-sharing) routes use extracts of Open Street Map for the selected region. An initial country-level map was generated to understand the boundaries of the catchment area in order to select a zoomed-in area for a more detailed calculation.
- Public transit routes use combinations of walking plus public transportation network present in the city (bus, metro, or short-distance rail). When available, regional public transit datasets
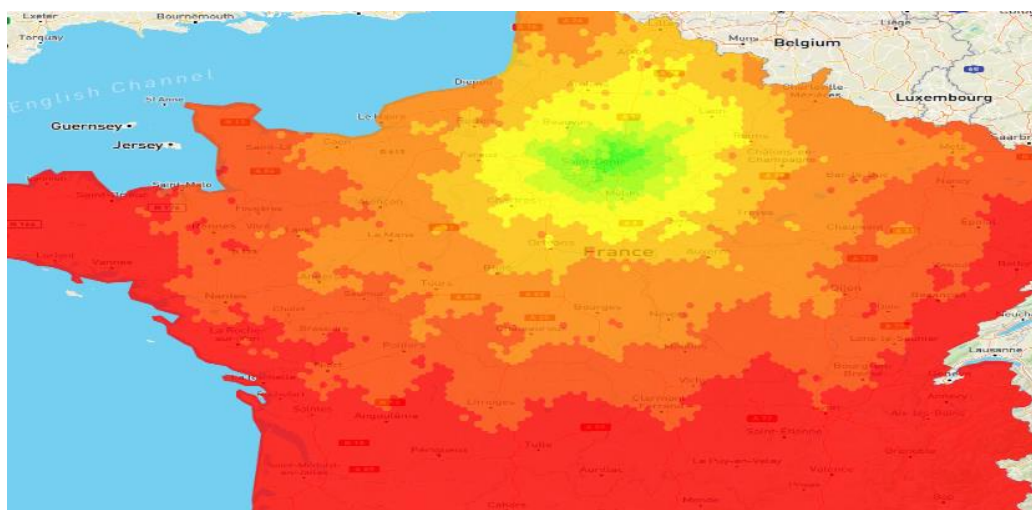
EUROPEAN PARTNERSHIP

Co-funded by the European Union

were integrated. Note that this also includes 'private' transit networks that operate direct shuttles to the airport.

The result of the calculation is a collection of catchment areas that indicate the average travel time calculated during day hours (6 AM-10 PM) and assuming optimal route selected for either vehicle or public transportation choice, for each point in the map. In aggregate, this creates concentric polygons representing the size of the region areas within a given travel time limit (e.g. within 1 hour). On one side, catchment areas for airports in the region were calculated (e.g. Figure 4- shows such catchment areas for the access to Paris CDG within its surrounding area).
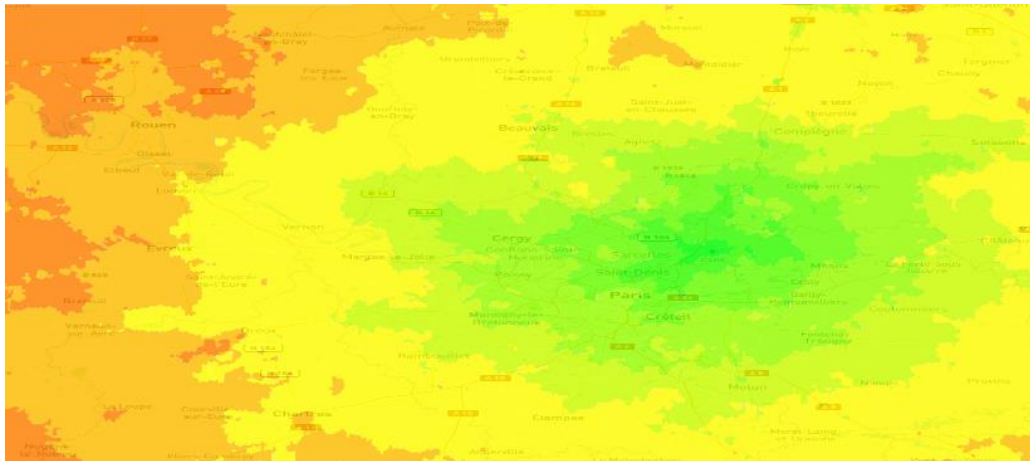
These results show how well-connected airports are to their surrounding area (catchment area), for different archetypes of airport and city. Expanded areas allow us to quantify how far around the region 'good connectivity' exists (below 90 minutes travel time – green and yellow area), including rural areas and other densely populated areas in the region. In general, it is noted that public transit networks play a major role in making a surrounding area accessible to the airport. This happens in archetypes 1-2, while archetypes 4-5 show much fewer connectivity options and to a smaller area. Archetypes 3 are in the middle as they are loosely integrated in the public transport network. Also, the transit network managed by the same country of the airport are well developed, but if the catchment area covers neighbouring countries, the transit times are much higher, even if distance remains relatively low. This is due to public transit networks not been sufficiently well connected between neighbouring countries. Private transit networks (direct shuttles) bridge some of these gaps but only within specific, dense areas (major cities in the region).

A good example can be found in public transit catchment areas for Belgian airports. The differences between BRU and CRL catchment areas can be assessed at a single glance, even though CRL has made important efforts to develop a private transit network of bus shuttles to all the main surrounding cities, from Lille and Bruges to Breda, Maastricht and Luxembourg.

(a)

EUROPEAN PARTNERSHIP

(b)

(c)

Travel time

🟩 < 10 min	🟩 10 - 20 min	🟩 20 - 30 min	🟩 30 -45 min	🟨 45 - 60 min	🟨 60 - 90 min	🟧 90 - 120 min	🟧 2 - 3 h	🟥 3 - 4 h	🟥 > 4 h
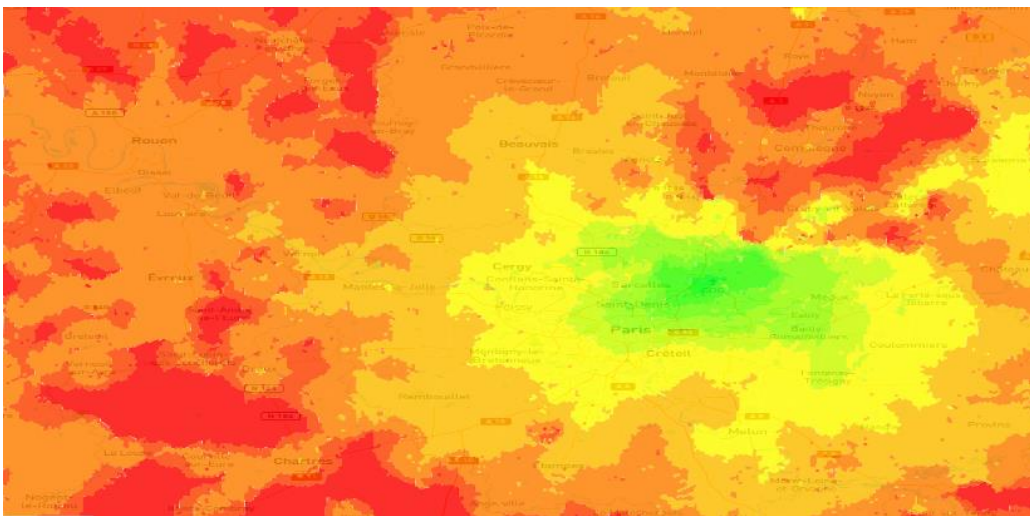
Figure 4: Example visualisations of a) and b) private vehicle transport, c) public transport to CD

EUROPEAN PARTNERSHIP

The BRU catchment area also shows the relatively high level of integration of Belgium's and the Netherlands' transit networks, whereas the integration with French and German ones is very low, see

Travel time

< 10 min	10 - 20 min	20 - 30 min	30 -45 min	45 - 60 min	60 - 90 min	90 - 120 min	2 - 3 h	3 - 4 h	> 4 h

Figure 5: Comparison of public transport catchment areas for a) Brussels and b) Charleroi airports

In addition, catchment areas for railway stations in the selected cities were generated following the same approach. Many cities have a single central station, while Paris is an example of urban environment with several major stations (see **Fehler! Verweisquelle konnte nicht gefunden werden.** which represents the catchment area for three Paris railway stations within their surrounding areas).

EUROPEAN PARTNERSHIP

Travel time

< 10 min	10 - 20 min	20 - 30 min	30 -45 min	45 - 60 min	60 - 90 min	90 - 120 min	2 - 3 h	3 - 4 h	> 4 h

Figure 6: Example of visualisation of door-to-platform travel time to major railway stations in Paris.

(a)

EUROPEAN PARTNERSHIP

Co-funded by
the European Union

(b)

Travel time

■ < 10 min	■ 10 - 20 min	■ 20 - 30 min	■ 30 - 45 min	■ 45 - 60 min	■ 60 - 90 min	■ 90 - 120 min	■ 2 - 3 h	■ 3 - 4 h	■ > 4 h

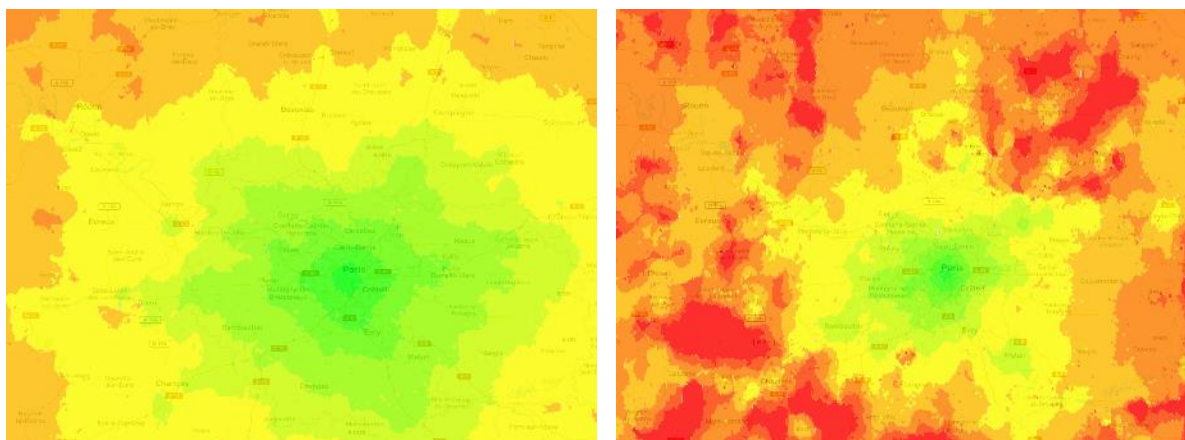**Figure 5: Comparison of public transport catchment areas for a) Brussels and b) Charleroi airports**

In addition, catchment areas for railway stations in the selected cities were generated following the same approach. Many cities have a single central station, while Paris is an example of urban environment with several major stations (see **Fehler! Verweisquelle konnte nicht gefunden werden.** which represents the catchment area for three Paris railway stations within their surrounding areas).
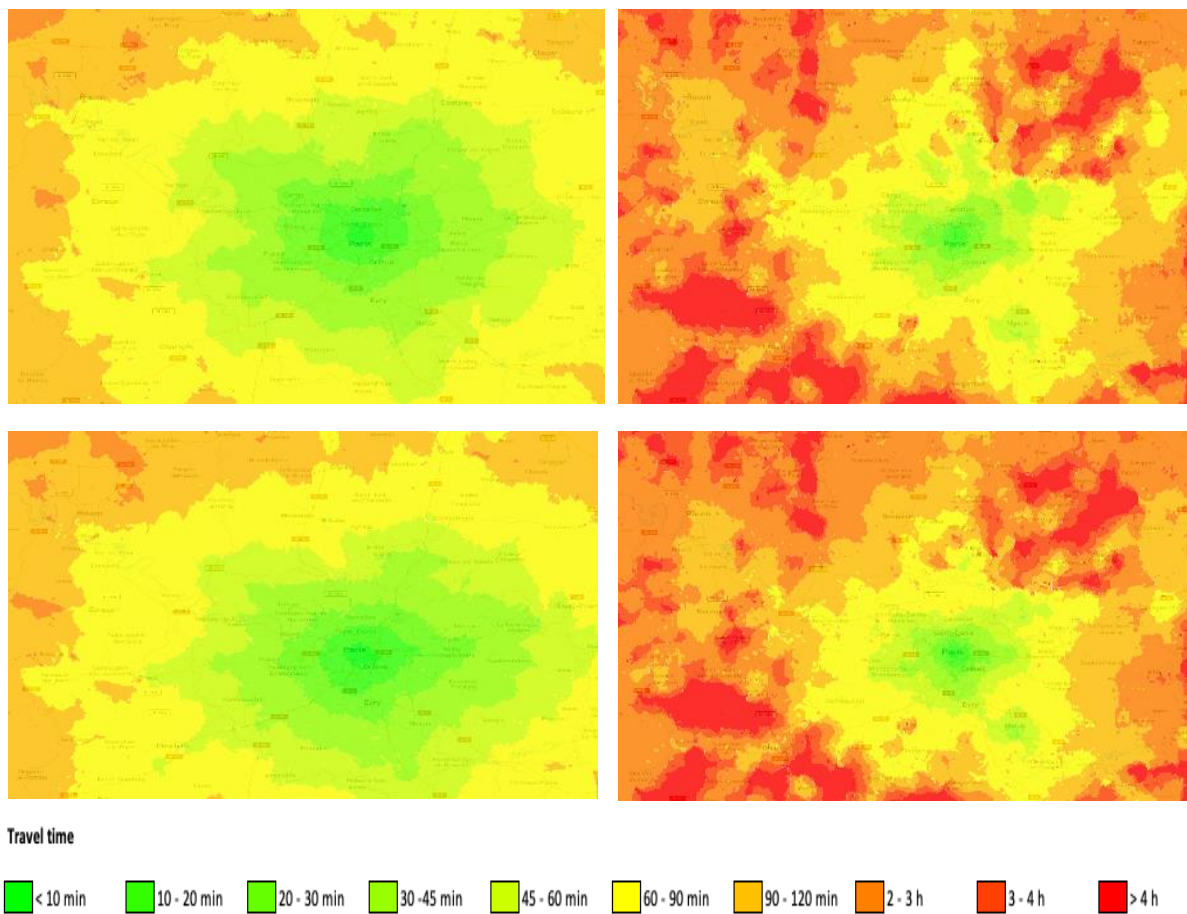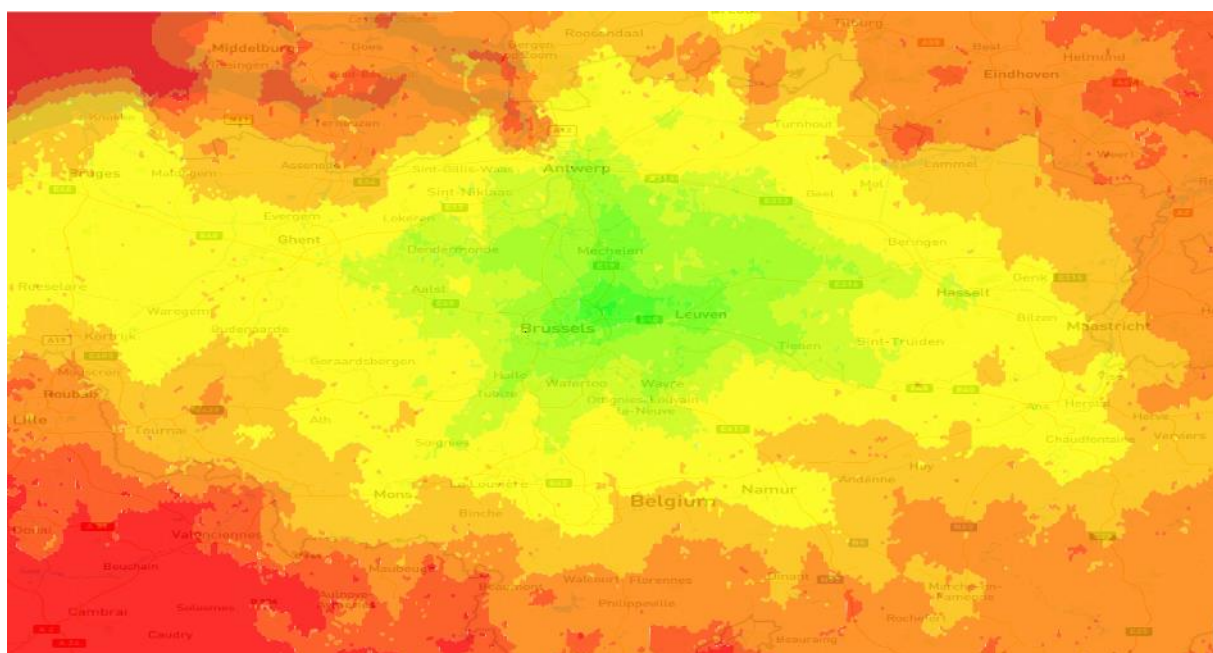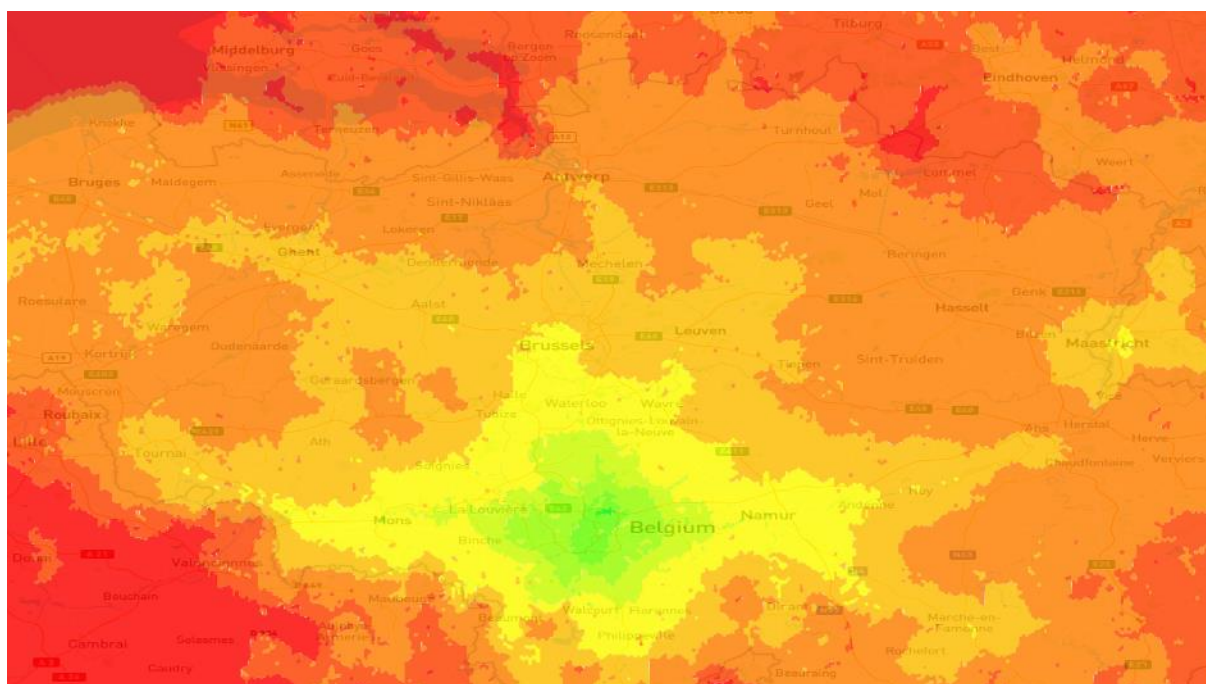
Private transport	Public transport
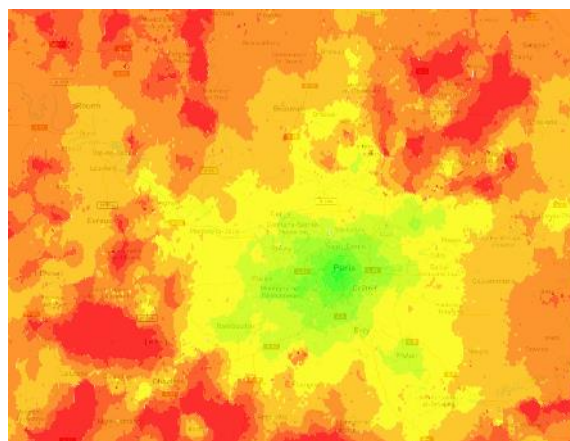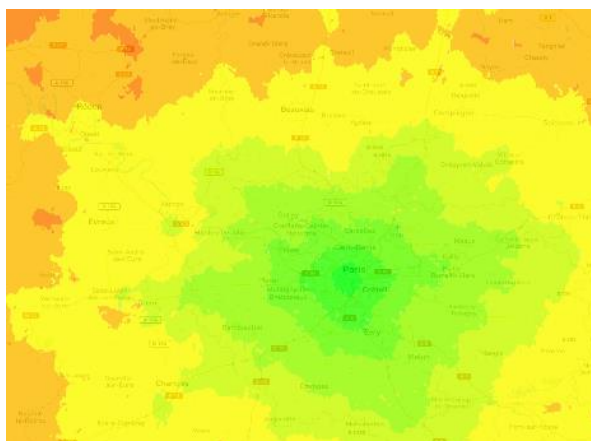
Montparnasse
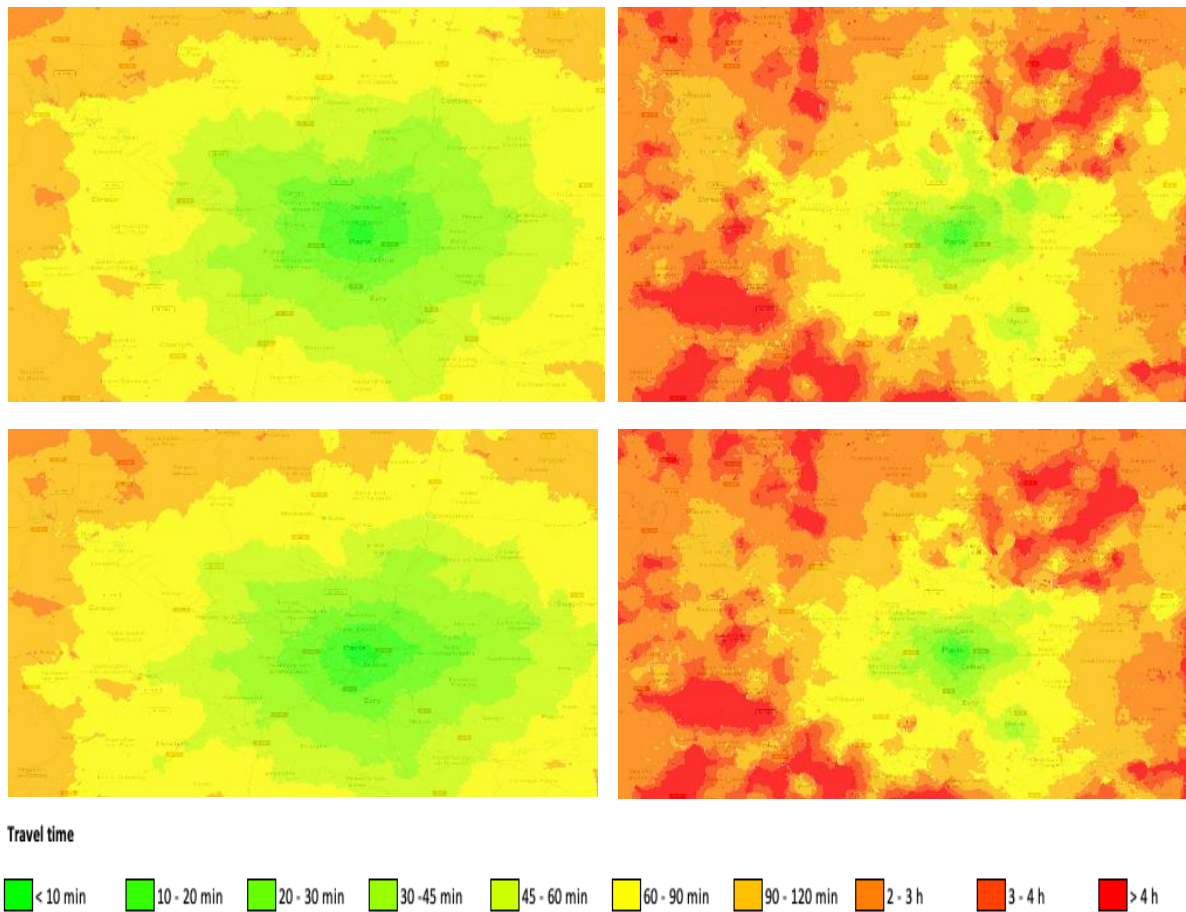
Figure 6: Example of visualisation of door-to-platform travel time to major railway stations in Paris

2.2.3.3 Generalisation of results to statistically represent travel time based on distance in cities considered equivalent to the archetype modelled

For its usability in the WP4 model, it is necessary to generalise the travel time (door-to-kerb) and create one function that represents each of the airport-city archetypes sampled. As a result, a travel time probability distribution is generated dependent on the population within the catchment area of a city-airport archetype. In order to sample the population within the catchment areas spatially, the population density of each city (obtained from GEOSTAT) is mapped over the travel time (door-to-kerb) calculated above. Figure 7 represents a map of the Paris region with GEOSTAT population density values.

EUROPEAN PARTNERSHIP
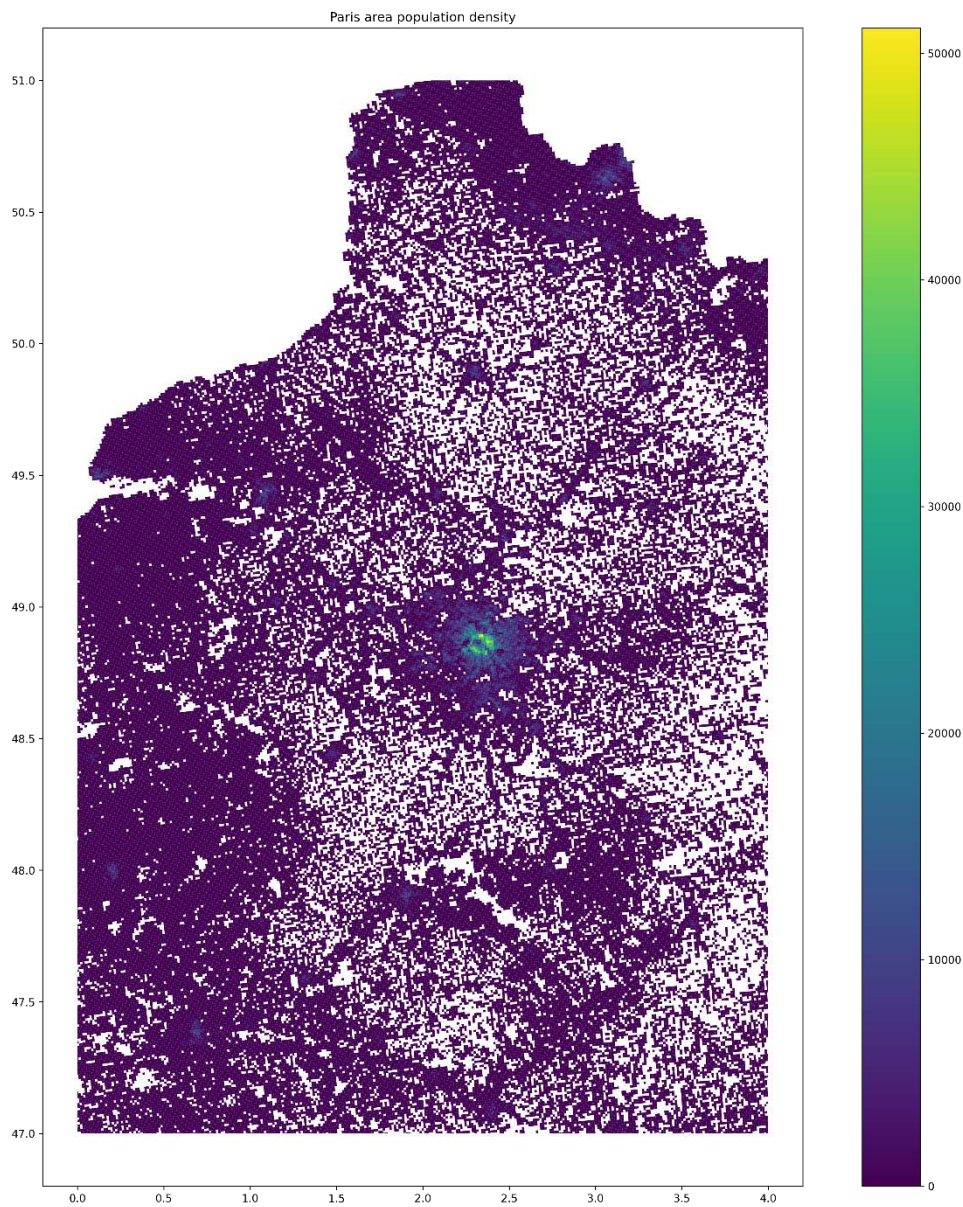
Figure 7: Example of GEOSTAT data visualisation of Paris region

Once the spatial sampling is done for each model city (one for each archetype) and transport type, the time distributions generated can be extended to new cities. To do so, a statistical distribution is fitted to the data to obtain a set of parameters that characterise that archetype (Figure 8).

EUROPEAN PARTNERSHIP
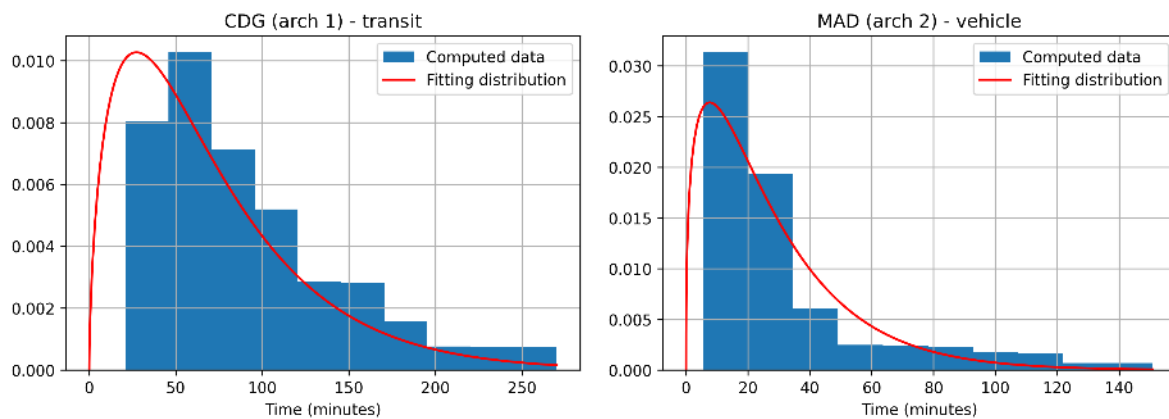
Figure 8: Fitting function for travel time distribution in selected airport-city archetypes

Given the shape of the obtained distributions, the best fit is a gamma distribution *f(x,κ,ϑ)* with two parameters *κ* and *ϑ*, with probability density function being:

$$f(x, \kappa, \theta) = \frac{1}{\Gamma(\kappa)\theta^{\kappa}} x^{\kappa-1} e^{-\frac{x}{\theta}}$$

Once the parameters are obtained for each archetype, every airport is mapped to one of the five categories. Then, the archetype's parameters are used in the probability density function to sample new values and obtain the door-to-kerb and kerb-to-door travel time values, presented in Table 7.

Table 7: Probability function parameters for city/airport archetypes

Archetype	Airport	City	Kappa - vehicle	Theta - vehicle	Kappa - transit	Theta - transit
1	CDG - LFPG	Paris	1.5	26.9	1.6	43.1
2	MAD - LEMD	Madrid	1.4	20.2	1.5	30.3
3	ARN - ESSA	Stockholm	1.9	20.5	1.6	22
4	CRL - EBCI	Brussels	5.9	9.4	9.5	12.4
5	BVA - LFOB	Paris	3.9	13.1	3.3	23.4

In addition, probability distribution functions are generated for each of the railway stations modelled in the selected cities. These are used in a similar way as for the airports, to calculate door-to-kerb and kerb-to-door times when the modal choice is rail. As a simplification, as introduced in Table 5, cities have been categorised as large (> 1 million population) and small (< 1 million population). The catchment areas used as representative are Paris and Stockholm, respectively. Table 8 shows probability distribution parameters for the city-rail archetypes.

EUROPEAN PARTNERSHIP

Table 8: Probability function parameters for city-rail archetypes

Archetype	Station	City	Kappa - vehicle	Theta - vehicle	Kappa - transit	Theta - transit
Large	Atocha	Madrid	1.3	25.3	1.3	37.1
Small	Central	Stockholm	1.3	34.7	1.3	33.5

2.3 Kerb-to-gate model

2.3.1 Process times

Once the passengers arrive at the kerb, they have to go through a set of processes on their way to the gate, where they can continue their journey by embarking on their flight. In the door-to-kerb stage, the socio-economic characteristics of the passenger are used to determine the probability of the transport mode used to reach the airport. In the kerb-to-gate stage, the socio-economic characteristics play more significant role, since the passenger's characteristics [8] are relevant to determine the time taken to go through the airport. A passenger with a more expensive ticket allowing fast access (e.g. fast-tracking security queues), or a frequent flying passenger that knows their way around the airport will undoubtedly spend less time to complete the steps required to reach the gate than someone who does not travel often and/or has a regular ticket. Therefore, the kerb-to-gate stage is divided in smaller actions [7], each of which is characterised by a time distribution, the parameters of which depend on the traveller archetypes (that is, their socio-economic characteristics). Another difference with respect to the door-to-kerb stage is that now we are not dealing with symmetrical stages: the kerb-to-gate and gate-to-kerb times are computed differently since they encompass different processes.

The processes involved in the kerb-to-gate (K2G) model are:

- kerb walk;
- luggage drop off;
- security;
- passport control;
- buffer allowed by the pax.

The processes involved in the gate-to-kerb (G2K) model are:

- baggage claim;
- passport control;
- kerb walk.

Therefore, for a given passenger archetype, the corresponding parameters will be used to sample from the distribution of each process of the kerb-to-gate and gate-to-kerb to obtain both times.

2.3.2 Passenger archetypes

The possible passenger archetypes, defined in D3.2 (Section 3) [10], are used to reflect the main type of passengers expected. They mostly contain information related to the socio-economic level of the

EUROPEAN PARTNERSHIP

Co-funded by
the European Union

passengers. One key feature is the frequency of travel, since it will impact the time taken to go through all the kerb-to-gate processes (the more frequent, the less time it takes them).

Table 9: Passenger archetypes

Characteristics (partly based on drivers identified in D3.1)	1) Business Flyer	2) Digital Gen Z Flyer	3) Environment-minded Flyer	4) Premium Flyer	5) Cultural Jetsetter	6) Holidayer	7) Golden Senior Flyer
Main motive of travel	business	mainly private	private & business	mainly private	mainly private	mainly private	private
Frequency of travel	frequently / very frequently	occasionally	occasionally	occasionally to frequently	occasionally to frequently	occasionally	frequently
Travel party size	1 to 2	1 to 2	1 to 2	up to 5 persons (family size)	1 to 2	single and up to 5 persons (family size)	1 to 2 (could also travel as part of organised travel group)
Burden (travelling with dependent people)	no	no	no	travelling with kids	no	travelling with kids	travelling with impaired companion
Booking/ Information gathering	online, travel agency (high-yield traveller)	online (high-yield traveller)	online (inflexible booking options)	in-person, travel agency (high-yield traveller)	online (inflexible booking options)	online (inflexible booking options)	in-person, travel agency (high-yield traveller)
Individual characteristics of users (criteria that define an individual)							
Predominant age group	18 - 65	15 - 70	15+	18+	15 - 65	30+ (with children under 15)	60+
Occupation	business or job-nomad (project work)	student, business, knowledge worker	student, business	business	student, business, knowledge worker	from low profile job to business	mostly retired
Category of salary / income	medium / high	high	medium	high	low / medium / high (more medium / high)	low / medium	medium

EUROPEAN PARTNERSHIP

Co-funded by the European Union

Characteristics (partly based on drivers identified in D3.1)	1) Business Flyer	2) Digital Gen Z Flyer	3) Environment-minded Flyer	4) Premium Flyer	5) Cultural Jetsetter	6) Holidayer	7) Golden Senior Flyer
Price elasticity	low (premium)	low (premium)	medium (premium /economy)	low (premium)	medium / high (premium)	medium / low (economy)	medium (premium / economy)
Household size	not relevant	1+	1+	from solo-traveller up to 5 persons (family size)	1+	from solo-traveller up to 5 persons (family size)	1 to 2
Psychological and sociological representations (travel needs that help to understand how profiles archetypes transport)							
Expected level of comfort	high	high	low	medium to high (premium)	medium	medium / high	medium
Degree of personalisation	high	high	high	high	low to medium	low	high
Technological affinity	high	high	low / medium	medium	high	medium	medium
Value of time	high	high	medium	medium	high	low	low
Further characteristics / requirements and values							
	working during travel	high digitalisation; environmental conscious	environmental conscious and act accordingly	high space requirements	travel as experience; environmental conscious	high space requirements	might need assistance

The information reflected in this table has been translated into specific parameters for each of the steps of travel. To model these stages, two distributions have been used, based on the previous work performed in [6].

The distribution used to model this set of processes is:

$$f(x; \frac{1}{\beta}) = \frac{1}{\beta} exp(\frac{x}{\beta}) + \beta$$

Where **x** is a continuous random variable and **β** is the **passenger parameter**. **β** is given in **minutes**.

Table 10: Exponential parameters

Passenger type	LuggageDrop	Security	Immigration	BaggageClaim	PassportControl

EUROPEAN PARTNERSHIP

Co-funded by the European Union

Business Flyer	0	4	1	0	4
Digital Gen Z Flyer	5	4	1	4	4
Environment-minded Flyer	0	6	1	0	6
Premium Flyer	10	4	1	4	4
Cultural Jetsetter	5	5	1	6	5
Holidayer	15	7	1	7	7
Golden Senior Flyer	15	9	2	9	9

The truncated normal distribution is similar to the regular normal distributions, but all the values are forced to be in the range [a, b], where a and b are parameters that we can set. For more information about the truncated normal distribution, see [11]. For this particular case, all the values are forced to be in the interval [0, 10] and the standard deviation is 60/3. The mean of the normal distribution (μ) is the passenger parameter. μ is given in minutes.

Table 11: Truncated normal parameters

Passenger type	KerbWalk	Buffer
Business Flyer	13	25
Digital Gen Z Flyer	13	30
Environment-minded Flyer	15	40
Premium Flyer	14	35
Cultural Jetsetter	15	35
Holidayer	25	40
Golden Senior Flyer	30	45

2.3.3 Ratio of passengers

These were not deployed in the previous Mercury modelling, so we have to create them from scratch, for Modus, as shown in Table 12.

EUROPEAN PARTNERSHIP

Co-funded by the European Union

Table 12: Passenger ratio parameters

Passenger type	Percentage of total[1]	Percentage of flexible in group[2]
Business Flyer	15%	75%
Digital Gen Z Flyer	10%	40%
Environment-minded Flyer	5%	5%
Premium Flyer	5%	75%
Cultural Jetsetter	15%	15%
Holidayer	30%	15%
Golden Senior Flyer	20%	25%

[1] Percentage of total: When simulating passengers, the ratio of appearance of each passenger type. This column will be normalised so the sum of all the percentages is 100%.

[2] Percentage of flexible pax in group: for each group, the percentage of passengers with a flexible ticket. This does not need to be normalised since some groups may have 0% of flexible passengers and others may have 100% (the percentages are independent among different groups).

2.4 Gate-to-gate model

The gate-to-gate stage begins when the boarding card is scanned at the departure gate and ends when the passenger enters the terminal at their final destination airport. Furthermore, this stage can include connecting flights and the procedures involved in this connection. The gate-to-gate component is the major component of the two simulation models Modus uses for the future transport passenger mobility assessment, and the source of major differences:

1. R-NEST[1] simulates three-dimensional routes traversed by flights, modelling the air traffic management (ATM) network with its associated performance indicators. The core is flight simulation within the EU-wide ATM network.

2. Mercury simulates individual flights and passengers transported. It includes a realistic cost model for the airlines, and passengers and their connections. Various processes are simulated, such as aircraft turnaround or passenger reaccommodation and thus the model can capture European-wide network effects especially on passenger mobility and connectivity [12].

As the cores and the end-results of the two simulation models are rather different, each model will be presented in a dedicated section. Mercury in Section 3, R-NEST in Section 4.

---

[1] EUROCONTROL's Research Network Strategic tool.

EUROPEAN PARTNERSHIP

Co-funded by
the European Union

3 Mercury passenger mobility model

3.1 Introducing the Mercury modelling context

As previously indicated, originally Mercury focused on the modelling of the gate-to-gate (G2G) phase of the passenger itineraries. Mercury is a stochastic agent-based model [12]. The model has been expanded to consider multimodal journeys. Figure 9 presents the different processes and data flows required to generate the input of the mobility model (with pre-computation of passenger itineraries, flight schedules, flight plans and rail alternatives) and post processing of the first-last mile processes. As indicated, the approach described covers all three phases of transport: with an strategic layer generating demand and supply flows and rail alternatives, a pre-tactical layer which translate those flows into individual schedules and passenger itineraries, and the tactical execution of the itineraries in the tactical layer.
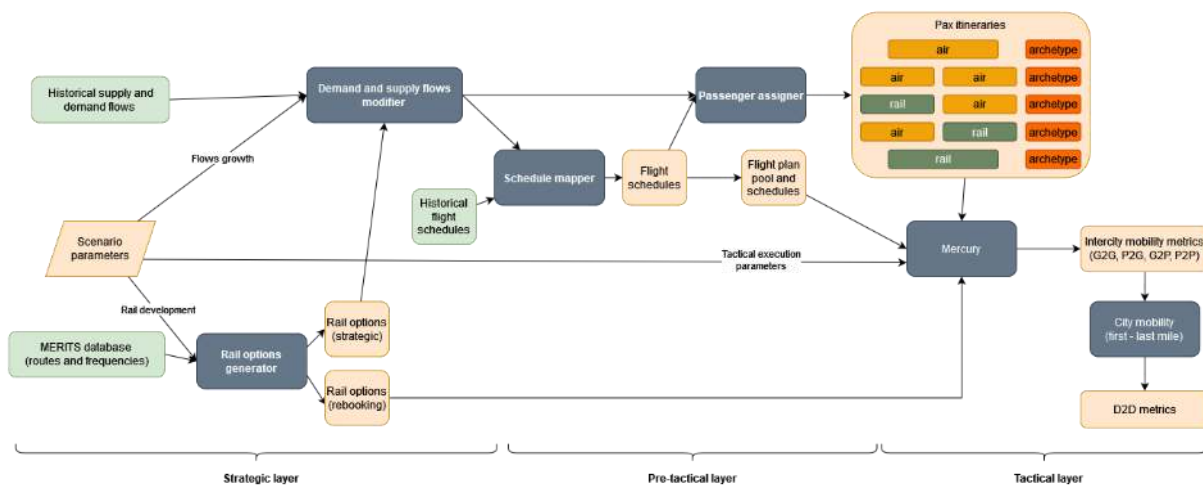
Figure 9: Mercury Modus implementation

Through the **demand and supply flow modifier** component the current supply of seats (i.e., flows) and passenger demand are grown to the future values and split between fully air, multimodal and rail itineraries. The outcome of this process is then used by **schedule mapper** (based on historical schedules) to produce future schedules. Note we need to ensure that possible flight plans are available for each schedule suggested. Then the demand flows is translated into individual passenger itineraries by the **passenger assigner** considering the available schedules. The outcome of this process is a set of passenger itineraries (indicating which flights and/or rail are used) along with their passenger archetype.

The Mercury model is then able to simulate the mobility of the passengers in the rail and air network. For the experiments where (severe) disruptions are modelled in the Paris and Madrid regions, rail is used as rebooking substitution alternative (see Section 0). The outcome of Mercury is then the intercity mobility metrics (gate-to-gate, platform-to-gate, gate-to-platform and platform-to-platform). The city mobility (first-last mile) model incorporates the travelling times required to access the travel infrastructure (door-to-kerb, kerb-to-gate, door-to-plaform, platform-to-door, gate-to-kerb and kerb-to-door processes), as explained in Section 2.

Each of the model components is explained in the sub-sections below, following the descriptions of the Modus scenarios and planned experiments.

3.2 Mercury scenarios and disruption

3.2.1 Overview of scenarios and parameters

There are four main Modus future scenarios (S1-S4), which are derived from high-level mobility objectives, existing scenario studies, and the work conducted within the Modus project. Note that whilst **S1-S3 will be modelled in Mercury**, the current plan is to model S4 using numerical methods, such as those presented in Section 1. The scenarios are briefly described below (for more details on the scenarios definition, please refer to D3.2 [10]):

Scenario 1 (S1), pre-pandemic recovery, is a future baseline against which the other three scenarios are compared. Within this scenario, it is assumed that the European transport market will recover to pre-crisis levels (2019) and that the air transport and railway network structure will remain similar to today. Furthermore, the implementation of innovative technologies, and market-based measures, will facilitate the reduction of emissions in the transport sector ([13], [19], [20]).

Scenario 2 (S2), European short-haul shift, envisions that the share of short-haul air traffic is replaced by cooperation between rail and air, which leads to a reduction in overall air traffic on short-haul routes in Europe. In this scenario, a high-quality transport network with HSR services on short-haul distances is established, and aviation services improve the coverage of long-haul routes. Scenario 2 assumptions include that by 2030 HSR traffic will double (this mainly concerns major links inter- and extra-EU) and that scheduled travel of under 500 km should be carbon neutral within the EU.

In **Scenario 3 (S3), growth with strong technological support**, high growth rates in the transport sector until 2040 are assumed, which significantly exceed those in the baseline scenario.

Within **Scenario 4 (S4), decentralised, remote and digital mobility**, a shift toward a more decentralised network is assumed. As forecast by the UN World Urbanization Prospects [18], the trend in urbanisation is not proceeding as anticipated in Europe, but the population has become more dispersed across rural and remote regions. These regions are becoming much more attractive due to enhanced options for remote working and virtual meetings. In line with the EU Smart and Sustainable Mobility Strategy [24], remote and rural regions will be better connected to the European transport network. This implies a significant increase in small and regional airports and additional railway stations in the network, moving towards a more decentralised (air) transport network structure. This is accompanied by the widespread implementation of technological innovations for regional aircraft.

The first three Modus scenarios have been refined during the project, especially with the view of modelling air and rail traffic growth, and passenger mobility evolution.

EUROPEAN PARTNERSHIP

Table 13: Key scenarios and parameters modelled in Mercury

Parameter domain	C1 (baseline - current)	C2 (short-haul ban - current)	S1 (baseline - future)	S2 (shorth-haul ban - future)	S3 (growth with technology future)
Air traffic	air flows in 2019[1]	air flows in 2019[1] minus the flights less than 500 km, in Germany, France, Spain, Italy	air flows 2040[2]	air flows 2040[2] minus the flights less than 500 km, in Germany, France, Spain, Italy	air flows 2040[3]
Rail traffic	rail traffic 2019	rail traffic 2019 plus shifted air traffic to rail on routes less than 500 km in Germany, France, Spain, Italy	rail traffic 2040	rail traffic 2040 plus shifted air traffic to rail on routes less than 500 km in Germany, France, Spain, Italy	rail traffic 2040
Average flight dep. delay	12.8 mins/flight[7]		7.5 mins/flight[8]		
Air emissions	current[4]		↓ by 7.5%[5]		
Rail emissions[6]	33g CO_2 / pax km (2021)		26g CO_2 / pax km (2030)		
Cooperation between air and rail	Please rail reaccommodation ratio, in Section 0				

[1] The traffic multipliers are used for C1, and C2, to grow supply and demand traffic from 2014 to 2019*.

[2] The traffic multipliers are used to grow supply and demand traffic from 2014 to 2017 and then further grow to 2040 using traffic multipliers for regulation and growth*.

[3] The traffic multipliers are used to grow supply and demand traffic from 2014 to 2017 and then further grow to 2040 using traffic multipliers for global growth*.

[4] Current aircraft emissions are based on BADA.

[5] Future aircraft emissions are estimated to be reduced by 5%-10% according to the ATM Master Plan [17]. A reduction of 7.5% is assumed.

[6] Rail emissions for current scenarios (C1, C2) are for 2021, based on [24], and for future scenarios (S1, S2, S3) are for 2030, based on [25].

[7] Sourced from PRR 2019 [26].

[8] Mid-range of Performance Ambition for 2035 [17].

* Air flows are generated by the flow modifier. See also Section 3.3 for details on (1)-(3).

EUROPEAN PARTNERSHIP

Co-funded by the European Union

In Table 13, key parameters used for modelling the three future scenarios S1, S2, and S3, as well as the two current baseline scenarios, C1 and C2 (for comparison purposes), are described. These will be refined and presented in further detail in D5.2.

- C1 (baseline-current scenario) represents 2019, and is used for comparing with S1 (baseline future scenario).
- C2 (baseline-current scenario with European short-haul ban), for 2019, is used for comparing with S2 (short-haul ban).
- S1 represents the baseline scenario, in 2040.
- S2 represents the European short-haul ban scenario, in 2040.
- S3 represents growth with strong technological support scenario, in 2040.

3.2.2 Modelling of disruption across scenarios

Disruption will be applied to all scenarios in Table 13. This will be modelled as bad weather at Paris (Charles de Gaulle and Orly airports) and Madrid (Barajas), at the same time. The disruption will be modelled as if advised to all impacted passengers the day before (D-1) and will operate (D) 0001-1400 (local time). The current plan[2] for the model is to cancel 90% of short-haul departures and 50% of long-haul departures, with all other departures delayed by 90 minutes. For the sake of model simplicity, arrivals into these airports will be assumed to operate as normal.

A rail reaccommodation ratio is defined as:

$$R_R = \frac{t_{rail\ recovery}}{t_{planned\ air}}$$

which describes the time that a recovered journey by rail (HSR or conventional mainline) would take, compared to the original journey planned by air (e.g. a value of 2 indicates that the journey recovered by rail would take twice as long as the originally planned trip by air). Under different scenarios, a threshold $T(R_R)$ for R_R will be set, such that only journeys with $R_R < T(R_R)$ will be recovered by rail – other such recovered journeys being deemed to take too long (having too high a disutility for the passengers). The conditionalities of passenger reaccommodation to rail are summarised in Table 14. Example recovery options for a given $T(R_R)$ are illustrated in Figure 10.

For the rail network, in the absence of any available capacity data (despite extensive attempts with the support of UIC (International Union of Railways, Modus partner) colleagues), no capacity constraints are assumed, whereas the capacity requirements are logged as part of the model outputs. Under scenario 3, higher rail frequencies are assumed and a higher value (both factors TBD) of $T(R_R)$ will be used, reflecting both higher service provision and a greater willingness/enablement to travel by rail, respectively.

---

[2] This may be revised during model calibration, and reported in D5.2. Flight disruptions might follow CODA data for similar types of event, for example.

EUROPEAN PARTNERSHIP

Co-funded by the European Union

Table 14: Conditionalities of passenger reaccommodation to rail

Conditionality	Pax (reaccommodation) action
Short-haul air AND $R_R < T(R_R)$	• random selection of pax decide not to travel and opt for voluntary reimbursement (most likely a rate of 20% of pax will be used, as per D3.2[16]) • split the remaining pax over the next three rail itineraries, using the waiting time function of Section 3.6.4
Long-haul air OR $R_R \geq T(R_R)$	• unaccommodated pax obtain ticket reimbursement recorded as a cost to the airline • long-haul pax do not switch to rail (modelling via another hub is too complex); a next day flight is assumed at no cost to the airline, except for the overnight accommodation cost

NB. Parameter values in this table are provisional and may be revised during model calibration, in order to ensure sensible model outputs and appropriate differentiation between the scenarios.
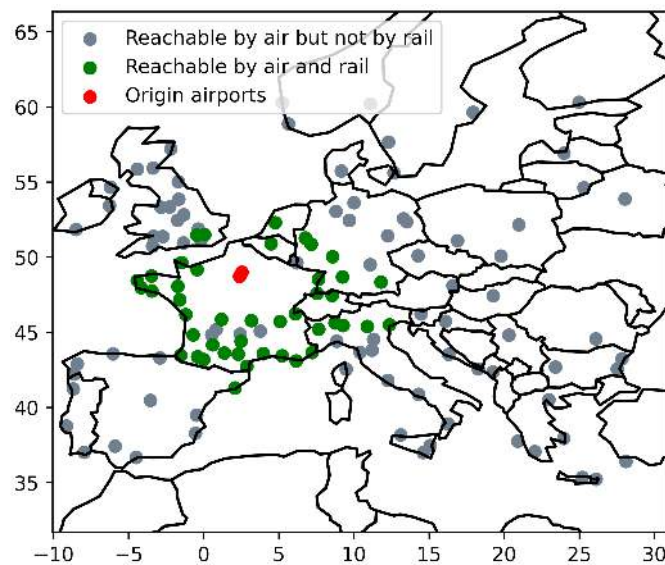
Figure 10: Direct air and rail connections from Paris

3.3 Flow and itinerary modifier

The demand and supply flows modifier component lies in the strategic layer, its role being to produce the future flows, and future passenger itineraries. Flows represent the future supply of seats, while passenger itineraries represent the future demand in an aggregated volume of passengers. The generated supply and demand volumes are varied across scenarios presented.
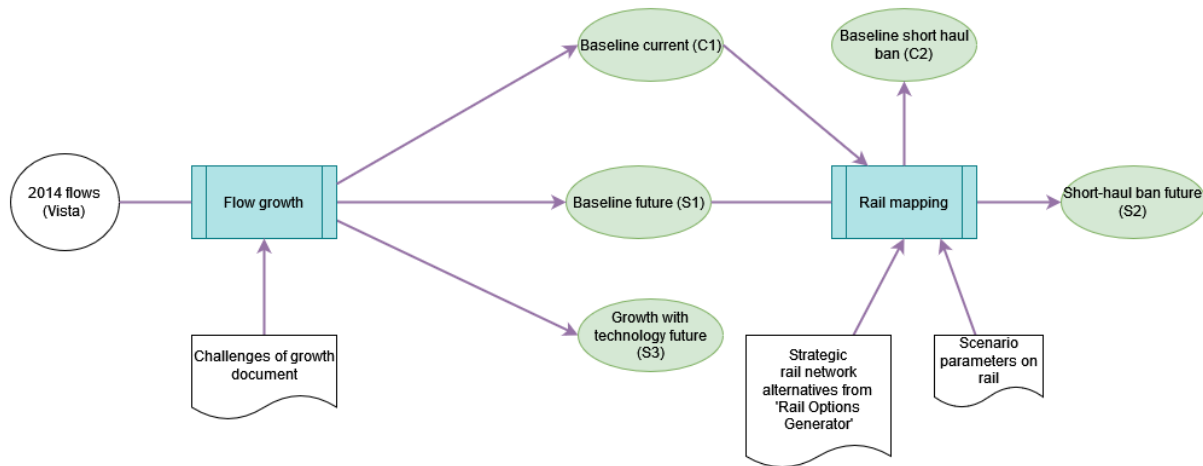
Figure 11: Depiction of flow and itinerary creation for Modus scenarios

In order to prepare the future flows and itineraries, we start from the historical (2014) flows and itineraries produced by the Vista project [14]. These are increased using EUROCONTROL's Challenges of Growth forecasts (2018) [13], more specifically using the traffic multipliers related to the appropriate forecast, and regional values of the specific flow/itinerary:

- for baseline current (C1) the traffic multipliers are used to grow both supply and demand for traffic between 2014 and 2019;
- for baseline future (S1) the traffic multipliers are used to grow both supply and demand for traffic between 2014 and 2017, and then using multipliers for Regulation and Growth forecast are grown to 2040 values
- for growth with technology future (S3) the traffic multipliers are used to grow both supply and demand for traffic between 2014 and 2017, and then using multipliers for Global Growth forecast are grown to 2040 values.

The traffic multipliers used can be found in tables in Annexes D and E of EUROCONTROL's Challenges of Growth (2018) Annex 1 [13]. Annex E contains traffic multipliers for ECAC states, while Annex D provides those for arrival/departure traffic between ECAC and outside regions. To obtain the 2040 traffic multiplier for non-ECAC regions, we use the average annual growth rate (AAGR) for the regions as depicted in Figure 12, and applying the formula:

$$regionmultiplier = \frac{2017}{2014} * (1 + AAGR)^{23}$$
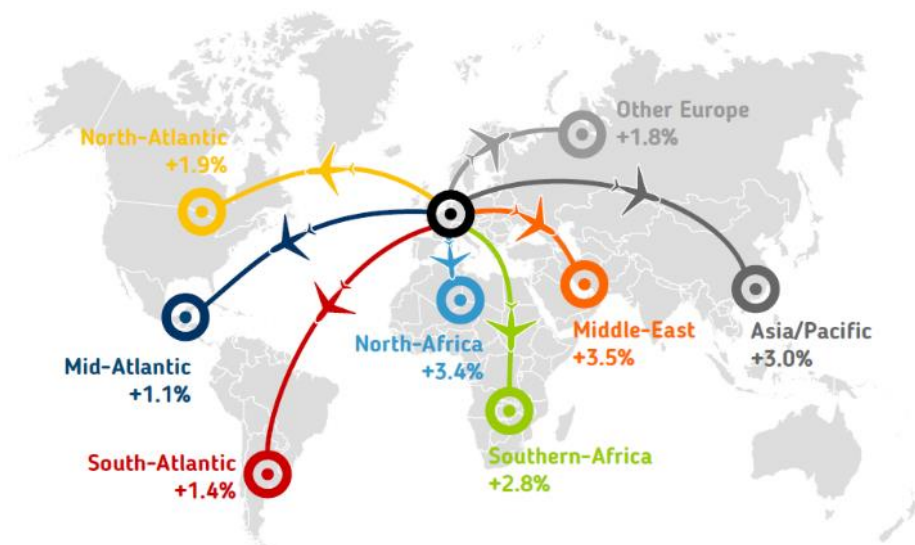
Figure 12: AAGR for main flows/itineraries for non-ECAC regions

(Source: EUROCONTROL's Challenges of Growth (2018) Annex 1 [13])

Having the traffic multipliers for ECAC countries and non-ECAC regions for the three scenarios (C1, S1 and S3), the scenario flows/itineraries are obtained by growing 2014 flows. Flows are represented as number of seats an airline offers between an origin and destination (OD) pair and aggregated number of passengers per itinerary and airline. The 2014 flows are then grown by the average of the multipliers for country/region of the origin and destination. Passenger itineraries are represented by groups of passengers travelling on the same itinerary (could be direct flight, or a series of flights), with the same airline, paying the same fare. The fare could be economy or flexible, thus distinguishing between passenger categories.

In order to obtain the flows/itineraries for the C2 and S2 scenarios, we need to overlay air traffic flows with the rail network. The analysis performed by the **rail options generator** in the rail layer (see Section 3.6) provides the different options available to passengers using rail.

Rail can be used as a substitution of air travel or as a segment, i.e., in multimodal itineraries. All flights with a great circle distance[3] lower than **500 km** will be considered as potentially replaceable by rail if the option exists. Demand flows which are only one-leg itineraries, i.e., only one flight, which overlap with a rail alternative would be considered as shifted to rail. For multi-leg itineraries, the **rail mapping process** depicted in Figure 11 will identify if the first or last leg can be performed by rail for a set of hub airports identified as where potentially multimodality can be performed. If that is the case, these segments will be moved to rail. The model will differentiate between railway stations in city centres and at airports, as the former will require the estimation of travelling time from platform-to-kerb. After this process, if for a given origin-destination all passenger demand has been shifted to rail, the supply,

---

[3] Orthodromic distance.

EUROPEAN PARTNERSHIP

Co-funded by
the European Union

i.e., seats on flights, will also be removed, i.e., the air link will be fully moved to rail. Finally, note that this strategic use of rail is only considered for rail routes within Spain, France, Italy and Germany.

3.4 Schedule mapper

The schedule mapper is based on the model developed in the strategic layer of the Vista model [14], and it produces the future schedules. The schedule mapper requires several inputs in order to generate future flight schedules:

- airport data;
- (historical) flight schedules;
- turnaround times, as the mapper adds not only the point-to-point flights, but creates rotations of added aircraft
- aircraft data (e.g. aircraft leasing prices, aircraft ranges), as new aircraft need to be added to the schedules;
- supply data (e.g. number of seats per origin-destination), which comes from the generated flows for Modus scenarios (C1, C2, S1, S2 and S3);
- airline data (e.g. type of airline).

For each scenario flow (created as described in the previous sub-section), the schedule mapper produces individual airline schedules and planned flight rotations.

3.5 Passenger assigner

The passenger assigner module creates future passenger itineraries. The passenger assigner requires several inputs:

- the future schedule generated by the schedule mapper;
- future itineraries, created in the flow modifier component, and reflecting requirements of the Modus scenarios;
- airport data (e.g. coordinates, minimum connecting times).

The passenger assigner considers actual seat capacity as provided by the schedules and connecting times. This means that not all passenger flows might be accommodated onto the flights and that some flights might end up with unrealistic low load factors. This is mitigated with the generation of synthetic passengers to ensure that operational factors are realistic in the model.

Only passengers that remain in the air mode will be assigned to the scheduled flights. In scenarios C2 and S2, the flows shifted to rail are removed from the air part – both from the flows and itineraries.

EUROPEAN PARTNERSHIP

Co-funded by
the European Union

3.6 Rail options generator

3.6.1 Setting the rail options generator context

A key part of this project is exploring the interconnectivity between air and rail. This multimodality is implemented through the development of a rail layer: a new layer of Mercury that allows us to exploit the MERITS database [5] and find rail alternatives to the scheduled routes. This can be done by a total substitution of air or through a collaboration of both means of transport.

The original schedules are defined by a series of airports. The most important ones are the origin and destination airports, but for journeys with multiple legs, intermediate airports also play an important role.

The output of this module is a set of rail-based metrics for each original air route that will be used to assess the viability of taking rail as a substitution of air routes. The main information generated, that will be later fed into the flow modifier and Mercury, are: average travel time, average waiting time, number of trains and time of the first and last train of the day. This is done for each original route.

3.6.2 Railway station-airport mapping

The first step towards adding rail options to the journeys is finding railway stations that can replace an airport. The criteria are based on distances: all the stations within 40 km of an airport are considered as candidates. Although there is often a main rail station that could be intuitively chosen as the replacement for the airport, reality is more complicated. By considering all the stations within range, the approach is more robust.
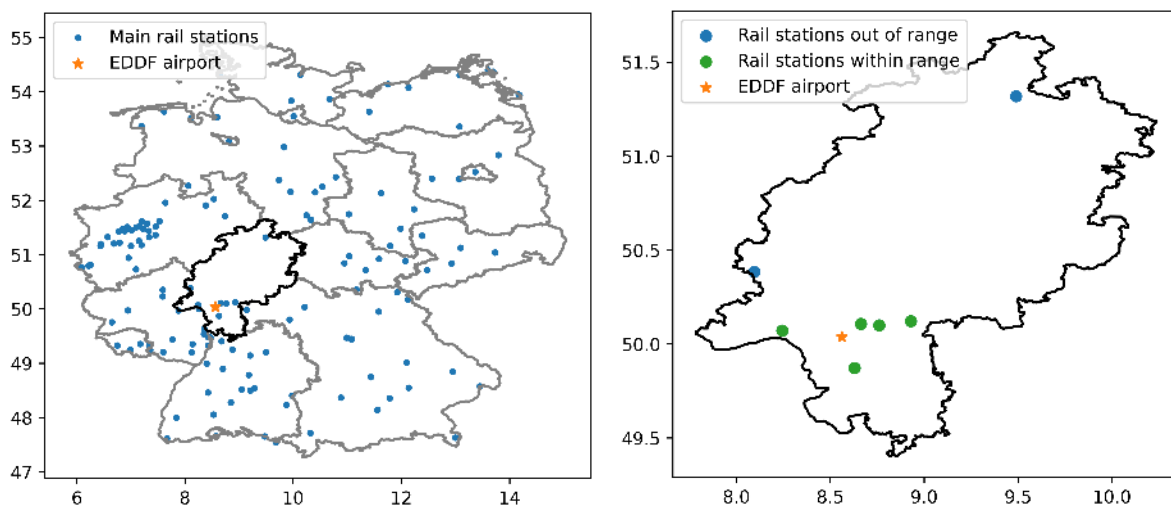

Figure 13: Railway station-airport mapping

EUROPEAN PARTNERSHIP

In some special cases, there are important airports that contain a train station at the airport itself. For these cases, that station will be considered as a different node, allowing us to compute travel times from the airport to the city centre or directly to other cities.

3.6.3 Rail data processing

Once the railway stations are assigned to the airports, the next step is to find existing rail routes to substitute the air routes.

Given the number of stations and all the possible rail routes, the options have been limited to direct connections.

Each route is determined by an identification code (ID). However, if the intermediate stops or the scheduled time differs, the ID is different. Therefore, each route has been processed to check whether it passes through any of the stations replacing an airport. Once this pre-processing is done, it is straightforward to extract all the trains connecting two given airports.

For each train, the time of departure from the origin and the time of arrival at the destination are obtained, and therefore the travel time. Then, by taking into account all the intermediate stops, the distance travelled can be computed with higher precision than just taking the (naïve surface) distance between the origin and destination. The average speed of the train is obtained from the previous metrics. This allows to classify the trains as HSR or conventional mainline.

3.6.4 Wait time estimation

Once all the trains connecting a pair of airports are identified and sorted by departure time, the wait time for a given train can be computed as $\Delta t_i = t_i - t_{i-1}$ where t_i is the departure time of the ith train (we will consider 0 the waiting time of the first train since the last train of the previous day and the first train of the following day are taken into account separately). Once the wait time of each train is computed, the mean and the variance are obtained with the general formulae:

$$\mu := \frac{1}{n}\sum_1^n x_i$$

and

$$\sigma^2 := \frac{1}{n}\sum_1^n (x_i - \mu)^2$$

where x_i would be Δt_i for this particular case.

The average wait time for a given origin and destination is computed as:

$$E(\omega) = \frac{1}{2}\left[\mu + \frac{\sigma^2}{\mu}\right] \geq \frac{\mu}{2}$$

Once all the information (average travel time, average wait time, first and last train of the day) is computed for each origin and destination that was originally covered by air, Mercury will add it to its inputs and determine the suitability of moving passengers to rail.

EUROPEAN PARTNERSHIP

3.6.5 Use cases

Once this layer is built, it can be applied to different subsets of the data to model different cases:

3.6.5.1 Strategic usage

In this case, rail is used as a substitution and complement of air itineraries, either fully as a replacement of the whole trip or as a feeder to/from the hub in a multimodal context.

For this purpose, a first filtering stage is implemented to identify the most suitable flights to be replaced by rail. As a threshold, we have selected 500 km (measured as the great circle distance between cities) as the maximum distance for a flight to be replaced by rail. Furthermore, we have identified four countries (Spain, Italy, France and Germany) to limit the study, given the development of their HSR network. For these countries, all possible origin-destination pairs that can be performed by rail, meeting the above-mentioned criteria, are identified.

As an extra step, we have also identified a set of eight airports that we have labelled as 'hubs' given the volume of passengers and the number of destinations that can be reached from them (they account for 58% of all connecting passengers for itineraries within the four countries considered). The possibility to perform multimodal itineraries will be limited to these airports:

- Madrid Barajas (LEMD)
- Barcelona El Prat (LEBL)
- Roma Fiumicino (LIRF)
- Paris Charles de Gaulle (LFPG)
- Paris Orly (LFPO)
- Frankfurt (EDDF)
- Munich (EDDM)
- Berlin Brandenburg (EDDB)

Two possibilities exist for these airports: either the rail station is located at the hub, or in the city centre. The strategic rail analysis differentiates between these two cases for each of the airports, e.g. identifying destinations which can be reached directly from LFPG and the ones that are reachable from Paris requiring the transfer of the passenger from the airport to the main rail station in the city. For these eight airports the multimodal segments described in Section 2 will be estimated.

This strategic rail analysis will be used by the flow modifier as described in Section 3.3.

3.6.5.2 Tactical usage

The tactical analogue of the rail layer use case was described in Section 0, i.e. on the common disruption applied to the Mercury scenarios.

4 R-NEST flight-centric network model development

4.1 Introducing the R-NEST modelling context

Most of the simulations related to ATM have been developed around microscopic and detailed models that allow the aircraft to fly precise three-dimensional routes. In this flight centric network study, the approach is more generic and can be defined as macroscopic with a high level of detail chosen in order to model the ATM network behaviour with its associated performance indicators.

The EUROCONTROL R-NEST tool focuses on the gate-to-gate flight phase, modelling the full flight trajectory and all the airside (i.e. airspace and route structures) and landside (i.e. airport) components of the European air transport network. For the Modus project, the model has been extended to encompass air passenger itineraries and rail journeys.

From the summer 2019 historical flight schedules, the air demand is expanded to the most-likely future level (i.e. for the year 2040). Then this flight demand goes through the rail layer and passenger itineraries model to compute the passengers travel time and to shift air demand to rail depending on the assumptions and rules of the simulated scenario.

Then R-NEST is able run the delay model, to detect and to solve the observed congestion at the network level by applying the Network Manager's mechanisms to respond to network constraints in a similar way to real operations.

The following sections describe the scenarios modelled in the R-NEST experiments, the modelling approach and the R-NEST components involve in the Modus simulations (i.e. air network delay model, passengers itineraries, rail layer).

4.2 Modelling approach

EUROCONTROL's R-NEST is retained to carry out the simulations. R-NEST is used as a research validation platform for prototyping and pre-evaluating advanced ATFCM concepts (e.g. SESAR). The model uses Network Manager data for long term ACC (area control centre) and ECAC network capacity planning assessment.

The approach adopted follows three main steps:

- Model calibration: to update (i.e. fine-tune) the R-NEST delay model and to measure reference network performance metrics.
- Future traffic sample: this phase uses the flight increase component within R-NEST to build the future reference traffic sample. Once future demand is built, R-NEST applies the passenger itineraries and rail layer rules to build a new air demand where a portion of the demand has been shifted to the rail according to the rules of the applied scenario.
- Performance assessment: for each scenario retained, simulation runs are performed to evaluate the impact of the high-speed rail development over the air traffic demand. Metrics are computed to allow comparison between the future scenarios against the reference and the baseline scenarios.

The following figure summarises the approach used for the modelling and assessment activities.
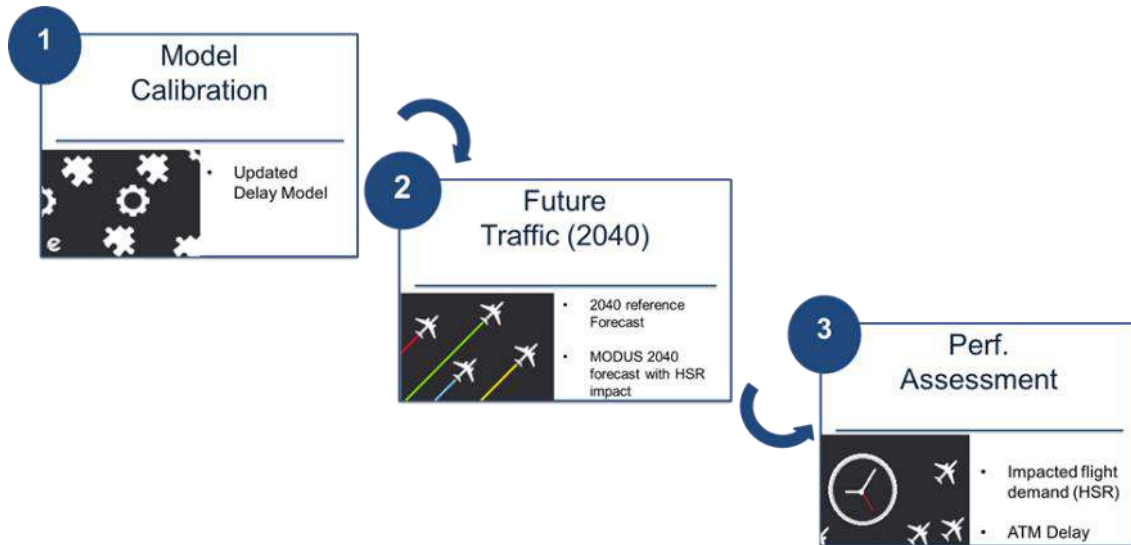
Figure 14: R-NEST modelling and assessment approach

The following sections describe the modelling approach steps.

4.2.1 Delay model calibration

The model calibration step serves to update (i.e. fine-tune) the R-NEST delay model and to measure reference performance indicators in order to compare and align actual impact with modelled impact of the traffic growth. The reference period in for the study is built from 61 days of traffic in (summer 2019) starting 01 August, ending 30 September.

Calibration is performed to reproduce the network delay situation during the summer 2019, as reported to the STATFOR CODA reports from August 2019 and used as reference (full month) ([22], [23]). During this period, the observed total delays (all causes) was 15.04 minutes per flight with 6.1 minutes per flight of primary flow management delays and 6.81 minutes and 2.13 minutes per flight, respectively for reactionary delays and non-ATFCM delays.

The next figure shows the breakdown of summer 2019 delays (all causes):
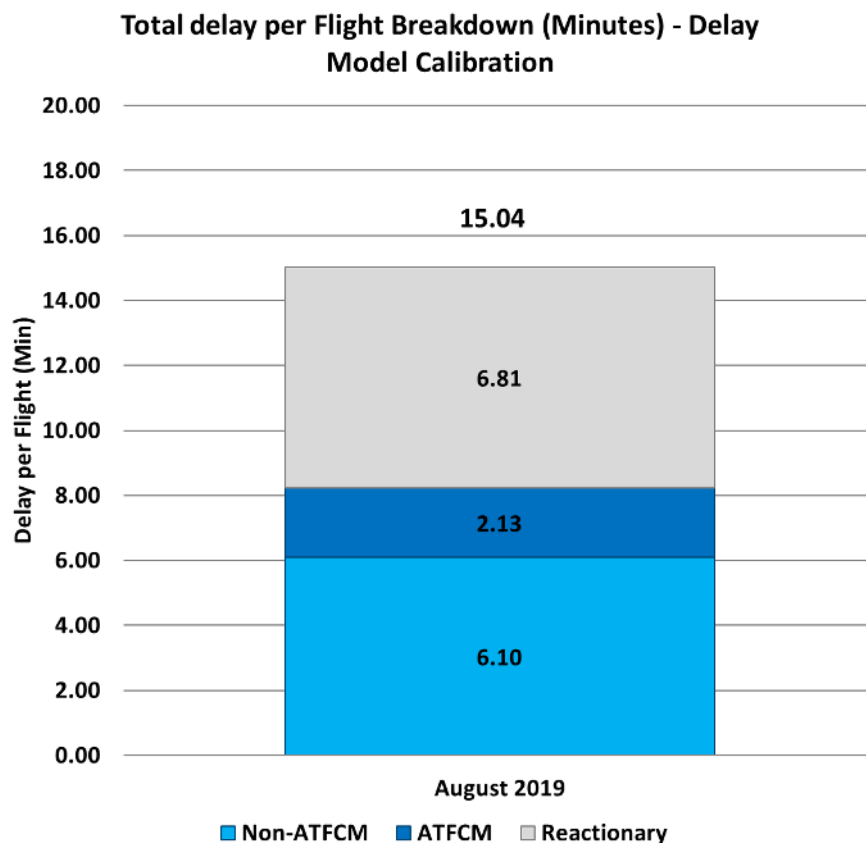
Figure 15: 2019 baseline summer delays (all causes)

(Source: STATFOR CODA [23])

4.2.2 Future traffic samples – the 2040 forecast

The R-NEST tool incorporates a module (FIPS – flight increase process) which allows future traffic samples to be created that completely respect the temporal distribution of the baseline sample (i.e. the same peaks are observed in the demand distribution at each airport) but take into account the planned airport hourly capacities.

Figure 16 illustrates the FIPS process.
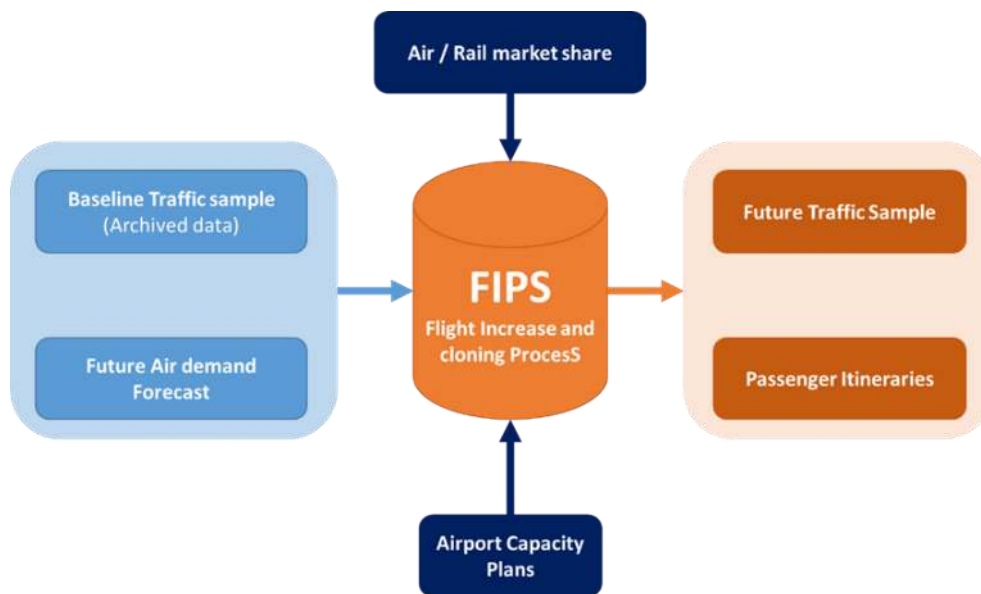
Figure 16: Flight increase and cloning process

Future traffic samples are constructed directly from the baseline traffic sample, which in our case is a 61-day period starting 01 August 2019.

2040 reference forecast

To build the 2040 reference air demand picture, growth figures, based on the latest EUROCONTROL Aviation Outlook 2050 (April 2022) [15], are applied to the baseline traffic sample, corresponding to the year 2040. We modelled two of the three scenarios: base (most-likely) and high.

In summary, by 2050, a 44% increase in traffic demand is expected in the base scenario. On the other hand, the high scenario anticipates a 76% increase.

EUROPEAN PARTNERSHIP
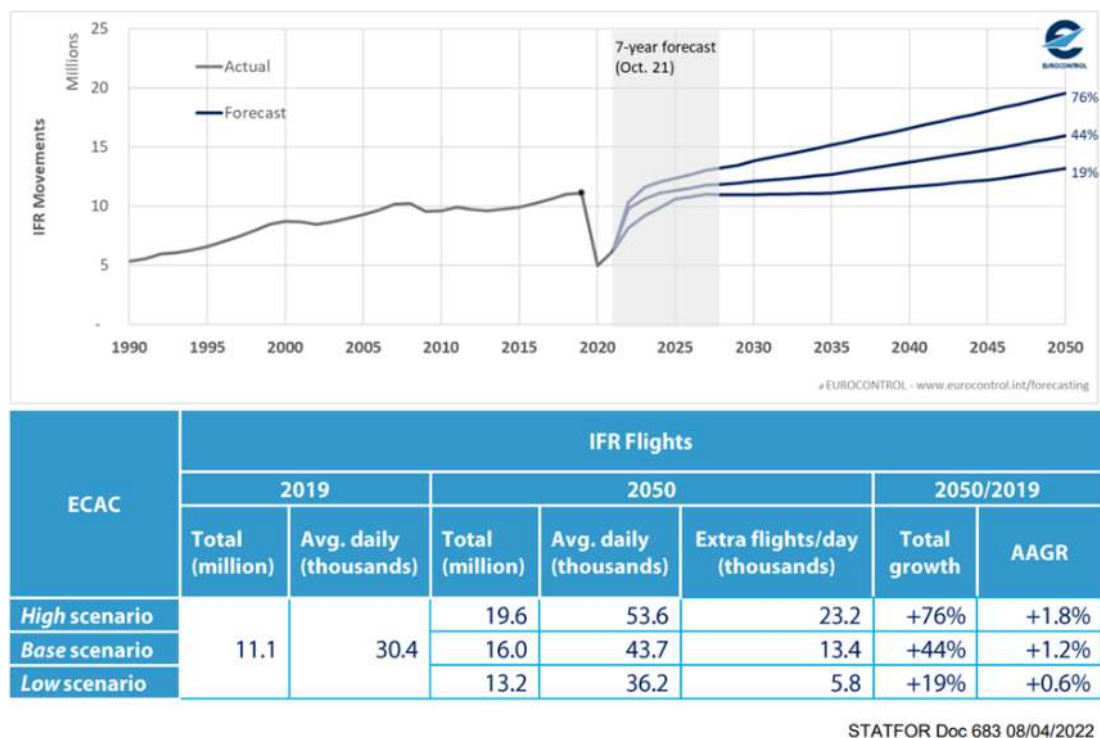
Figure 17: EUROCONTROL's 2050 forecast summaries

(Source: EUROCONTROL Aviation Outlook 2050 [15])

For the year 2040, the expected demand will not be so high, the corresponding growth rate are respectively of +25% for the base scenario and +51% for the high scenario.

4.2.3 The network performance assessment

The network performance assessment is performed by running the R-NEST delay model for all the modelled scenarios. R-NEST simulates full days of traffic demand at the European geographical level, monitoring the emergence of disruptions across the network (i.e. airspace or airport capacity shortfall) and resolving them by applying the Network Manager mechanism to solve them by regulating the demand. R-NEST propagates the primary flow management delays across the network in order to track the reactionary delays all along the simulated days.

Figure 18 illustrates the delay propagation during a day of operations.

EUROPEAN PARTNERSHIP
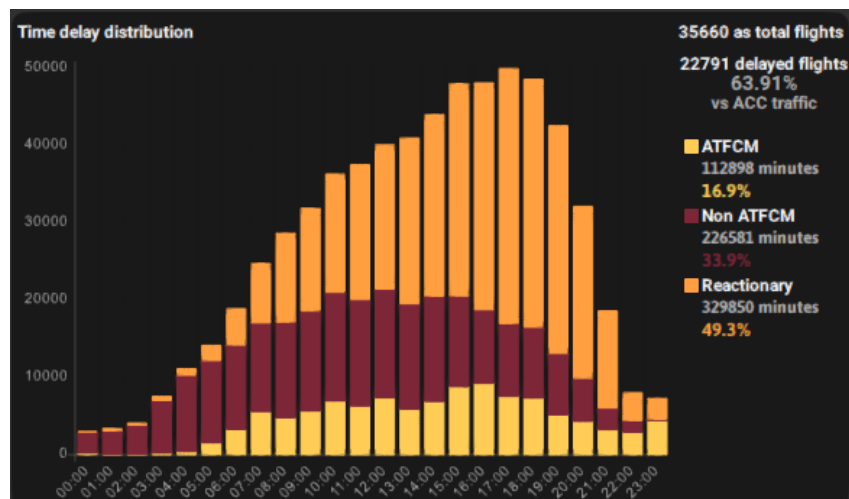
Figure 18: Delay propagation

The R-NEST network delay model description is detailed in the next section.

4.3 R-NEST scenarios

Four main scenarios have been identified for Modus, as described in Section 3.2.1, three of which will be simulated in Mercury. These first three scenarios have been refined in view of the modelling of passenger mobility evolution, air and rail transport network (current and future).

Correspondingly, therefore, three main scenarios and four sub-scenarios, described below, will be modelled in R-NEST to explore the impact of high-speed rail development on air transport:

- R1, baseline scenario (cf. S1): represents the air network situation in the year 2019. It serves as calibration reference for the air network delay model and it is used for comparison against future scenarios.
- R2, reference scenario: this scenario describes the 2040 situation, based on most-likely growth assumptions for transport mode.

    o R2.1, short-haul ban (cf. S2): in this sub-scenario, short-haul traffic is replaced by rail connections. Flights less than 500 km in Germany, France, Italy and Spain are shifted to rail routes.
    o R2.2, short-haul ban and travel time competition: this sub-scenario extends the short-haul flight ban by shifting all flights where rail competition presents a time travel gain.

- R3 high reference scenario (cf. S3): represents the 2040 picture assuming strong growth for transport mode.

    o R3.1, short-haul ban: similarly, to R2.1, short-haul traffic is replaced by rail connections.
    o R3.2, short-haul ban and travel time competition: same assumptions as R2.2 applied on the strong growth scenario.

Co-funded by the European Union

Table 15: Summary of the R-NEST scenarios

Scenario	Air	Rail
R1 (baseline scenario)	2019 traffic level	2019 rail network
R2 (reference scenario)	2040 most-likely scenario (base traffic growth)	Future rail network
R2.1 (short-haul ban)	2040 most-likely scenario traffic level minus shifted air demand to rail on routes less than 500 km in Germany, France, Spain and Italy	Future rail network
R2.2 (short-haul ban & travel time competition)	2040 most-likely scenario traffic level minus shifted air demand to rail on routes: • Less than 500 km in Germany, France, Spain and Italy • With air/rail competition and routes with lower door-to-door travel time for rail	Future rail network
R3 (high reference scenario)	2040 high scenario (high traffic growth)	Future rail network
R3.1 (short-haul ban)	2040 high scenario traffic level minus shifted air demand to rail on routes less than 500 km in Germany, France, Spain and Italy	Future rail network
R3.2 (short-haul ban & travel time competition)	2040 high scenario traffic level minus shifted air demand to rail on routes: • Less than 500 km in Germany, France, Spain and Italy • With air/rail competition and routes with lower door-to-door travel time for rail	Future rail network

NB. Once the final parameterisations of the Mercury and R-NEST models are concluded, a comparison table between the two will be presented in D5.2, to support the interpretation of the corresponding results. To the greatest extent possible, the two sets of scenarios have been aligned, although each faces particular constraints (e.g. the absence of full D2D passenger itineraries in R-NEST and of higher resolution airspace structures in Mercury).

4.4 Modelling the rail layer and passenger itineraries in R-NEST

The development of HSR connections that have obvious time travel benefit, as well as the renewed interest for night trains that could be easily operated on current rail infrastructures across the world, lead to more passengers opting for such mode of transportation, impacting the flight demand.

Co-funded by
the European Union

The evaluation of this impact over the ATM network performances in terms of flight demand and delays is the main purpose of the flight centric network study. In order to do so, extensions of the simulation capabilities of the R-NEST tool are needed to encompass passenger itineraries and to integrate a rail model with future HSR connections. The following sections describes the passenger itineraries and the rail model.

4.4.1 Air passenger models

A passenger journey model, used to compute the various travel times for a passenger between origin and final destination, via departure airport and the arrival airport, using the city archetypes is implemented in R-NEST.
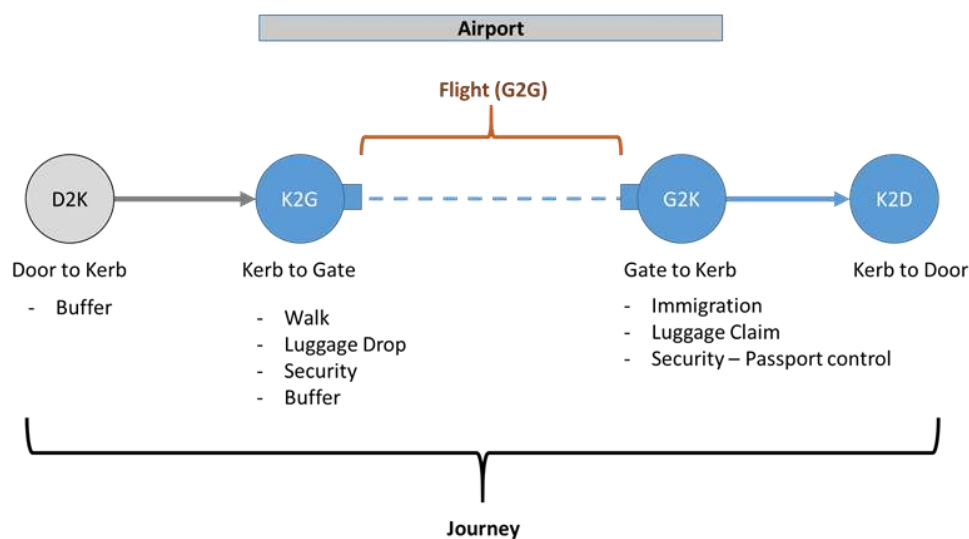
Figure 19: Stages modelled for air travel

All journey phases are modelled:

- Door-to-kerb (**D2K**): moving to the airport (by car or public transport)
- Kerb-to-gate (**K2G**): sequence within the airport
- Gate-to-gate (**G2G**): the flight
- Gate-to-kerb (**G2K**): to exit the airport
- Kerb-to-door (**K2D**): from the airport to the final destination

A generic model (see Section 2.2.2 on synthetic data on city archetypes for the development of the D2K model), is used to compute the travel time between home to departure airport (D2K) and destination airport to final destination (K2D).

For the K2G and G2K legs, reference values from the DATASET2050 study [6] will be used for the main European airports:

EUROPEAN PARTNERSHIP

Airport	D2K	K2G	G2G	G2K	K2D	D2D
EDDF (Frankfurt)	0H36	2H15	2H17	0H37	0H30	5H58
EDDM (Munich)	0H56	1H55	2H11	0H33	0H48	6H00
EGKK (London Gatwick)	1H00	2H05	2H31	0H34	0H52	6H28
EGLL (London Heathrow)	1H10	2H15	2H21	0H36	1H00	6H37
EHAM (Amsterdam)	0H40	2H15	2H21	0H37	0H36	6H10
LEBL (Barcelona)	0H50	2H05	2H29	0H33	0H44	6H21
LEMD (Madrid)	0H45	1H54	2H27	0H32	0H37	6H04
LFPG (Paris CDG)	1H00	2H15	2H15	0H37	0H53	6H21
LFPO (Paris Orly)	0H55	1H56	1H53	0H33	0H47	5H37
LIRF (Rome)	0H57	1H55	2H12	0H32	0H49	6H02

Figure 20: DATASET2050 travel stage reference values

(Source: DATASET2050 [9])

For other airports, average values, will be deployed:

- **K2G**: 1 hour 54 minutes;
- **G2K**: 31 minutes.

The door-to-door passenger journey model allows R-NEST to evaluate a door-to-door travel time for all air passengers, assuming 80% will use public transport and the remaining 20% will use private vehicles.

Figure 21 illustrates the function for the travel time statistical distribution for each city archetype.

EUROPEAN PARTNERSHIP
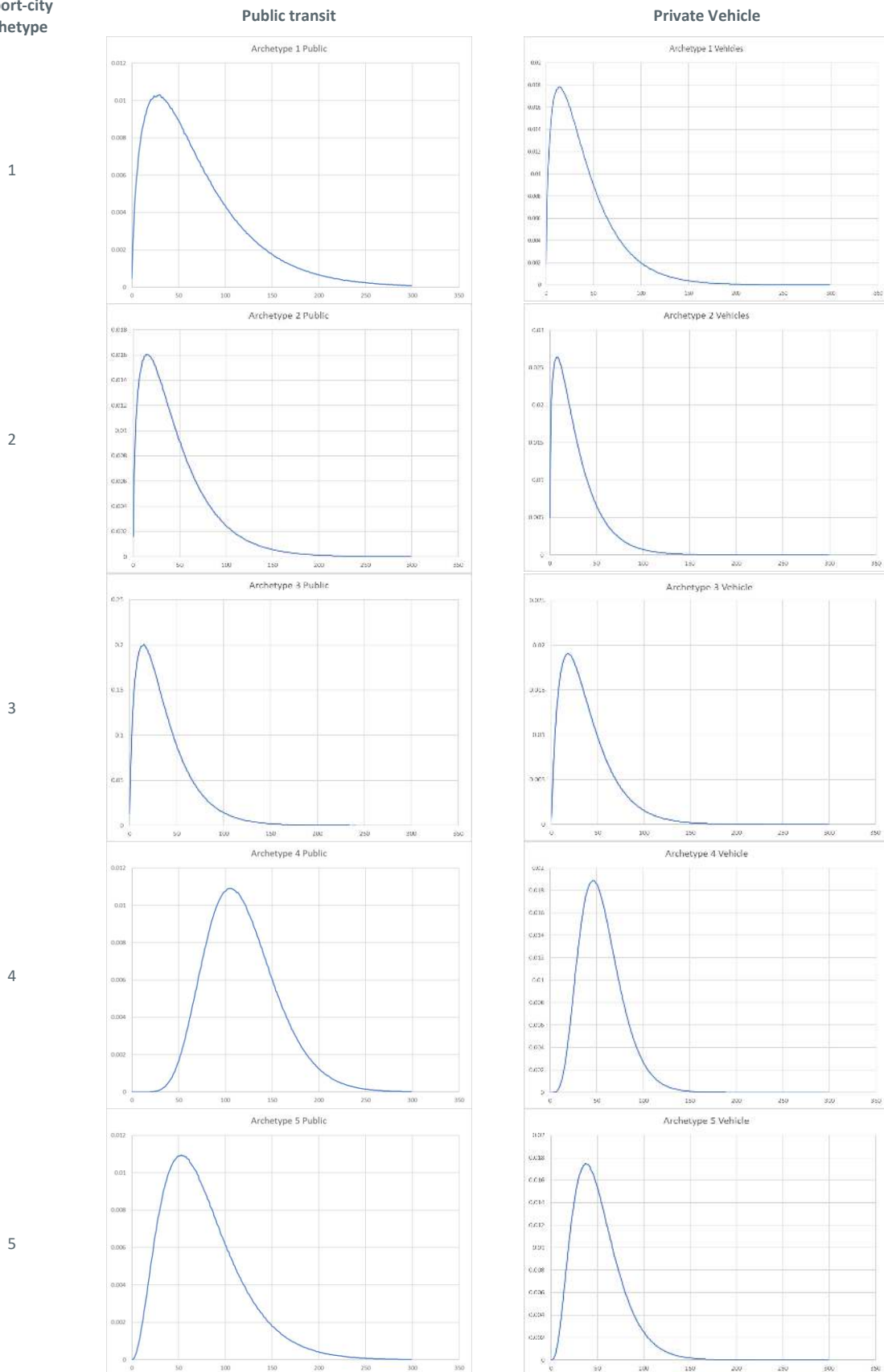
Figure 21: Travel time statistical distribution for each airport-city archetype

EUROPEAN PARTNERSHIP

4.4.2 The rail journey model and the impact on air traffic demand

A rail journey model is introduced in R-NEST, allowing the comparison of air and rail passengers total travel times for same city-pairs.
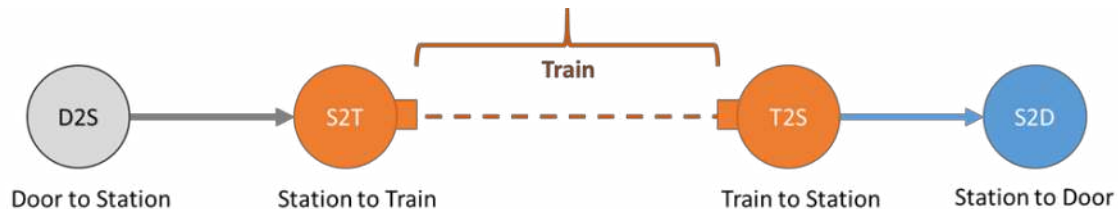
Figure 22: Stages modelled for rail travel

To allow the door-to-door rail travel time computation, average values based on observed public transport time in main European cities (i.e. Paris and Madrid), have been retained.

The values corresponding to each rail journey's leg are:

- Door-to-station and reverse (**D2S**, **S2D**): 45 min;
- Station-to-train (**S2T**): 30 min;
- Train-to-station (**T2S**): 20 min.

The identification of the train stations, the type of train (normal or HSR) is based on the exploitation of the MERITS data.

Rail impact over air demand

To evaluate the impact on high-speed rail (HSR), two mechanisms will be introduced:

- **Flight ban policy**: for flights below 500 km (great circle distance between airports), limited to city-pairs with air-rail competition;
- **Air-rail competition**: for all passengers, total travel time is computed for both air and rail transport modes. Flight passengers will switch to rail mode when a one-hour travel time benefit is observed for the rail mode compared to air. When 20% or more of an aircraft's passengers transfer to the rail mode, the airline will cancel the flight.

The 'flight ban policy' and the 'air rail competition' strategies will be applied on the reference 2040 air demand forecasts (i.e. base and high scenario), resulting in a number of flights being transferred from air transport to rail.

4.5 Air network delay model

The air network becomes congested when, to accommodate the traffic demand, a number of airports or airspaces (i.e. controlled sectors) operate simultaneously close to their peak capacity.

The modelling of the air transport network is carried out by using the R-NEST tool (with closely analogous functionalities supported in Mercury, as reported in [12]). To simulate one day of operations, the tool combines the expected flight demand and the available airport and en-route (i.e. airspace) capacity. The tool emulates network operations and allows us to observe the appearance and propagation of delays that characterise the degradation of network performance. Those delays can result from capacity shortfalls within the network infrastructure (ATFCM), or be caused by events external to the network (non-ATFCM). As a knock-on effect, the delays can follow one aircraft all along the day of operations (reactionary).

Delays have been classified as:

- primary, delays to this flight;
- reactionary, knock-on delays incurred by this aircraft on previous flights.

Primary ATFCM delays are captured by the R-NEST network delay assessment model. The tool emulates the CASA (Computer Assisted Slot Allocation) algorithm used by the Network Manager to respond to network constraints, so R-NEST regulates traffic in a similar way to real operations.

Primary, non-ATFCM delays are mostly generated by internal disturbances, related to the intrinsic variability associated to air traffic processes (e.g. handling, passengers or baggage problems). Internal disturbances have been modelled by using a probabilistic model developed from CODA data. To model internal disturbances:

- all delays are taking place on the ground;
- an empirical distribution of the minutes of delay has been built;
- based on the observed probability of occurrence (i.e. 25%), a random delay value is applied to the flights;
- this random delay cannot be lower than 5 minutes and cannot exceed 30 minutes. The average is calibrated to match delays in the baseline 2019 dataset.

Reactionary delays are incurred by delays affecting previous flights and using the same aircraft. It is through reactionary delay that problems at one airport propagate through the network.

To capture the level of reactionary delay we have linked the flights using the following algorithm:

- for every flight, a check on the aircraft registration or flight number has been made. A link for the flights with the same registration number has been made;
- for the rest of the flights, a search is performed at the destination airport for the next departing flight checking the aircraft type, the operator and taking into account a specific average turnaround time per airport or airline. If no information is available for turnaround time at destination airport, an average value of 53 minutes is used;
- when linked, a rotation margin is evaluated to assess if the initial delay can be absorbed before the next scheduled flight rotation.

After running the algorithm, 90% of the flights have been linked.

The figure below illustrates the reactionary delay mechanism implemented within the R-NEST tool, and the effects of the rotation margin on initial delay.

For this study, modelling has focused on delays at airports rather than in the airspace.
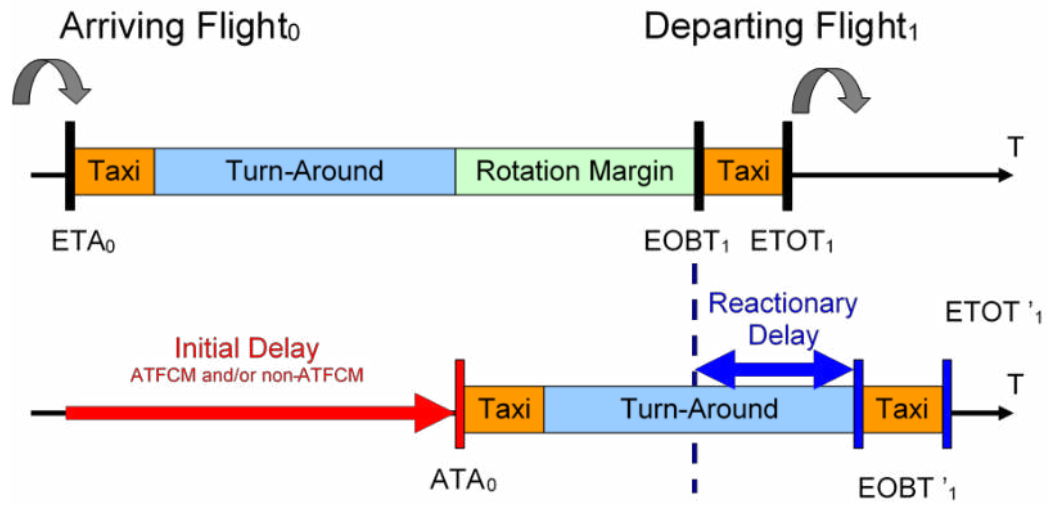
Figure 23: The R-NEST tool reactionary delay mechanism

5 Conclusion

The work presented in this deliverable provides an approach in order to improve the door-to-door travel concept through integrated air and rail modelling. Towards that, passenger mobility model (Mercury model) containing two sub-models, i.e. Schedule mapper in the strategic layer and passenger assigner in the pre-tactical layer are further improved to reflect the multimodality concept. The modelling approach presented in here is based on a set of diverse scenarios, where each requires specific changes to the aforementioned sub-models, as well as adding two new sub-models in the strategic layer. The additional new sub-models, i.e., flow modifier generates the future flows and future itineraries based on each scenario , while rail-option generator is added to produce rail alternatives for the cancelled flights or as a feeder to/from the hub in a multimodal concept. The work presented here is also based on the city archetype concept which is defined as a combination of air and rail transport mobility of NUTS3 regions. The building of joint city archetypes removes being tied to specific constraints at a particular airport/ rail stations and therefore, allow us to consider the movements between two regions more holistically. Finally, alongside the further development of passenger mobility models, the EUROCONTROL flight-centric network model R-NEST is extended to encompass air passenger itineraries and rail journeys. The simulation results of Mercury and R-NEST models are reported in Deliverable 5.2.

EUROPEAN PARTNERSHIP

6 Next steps

This deliverable has presented the methodologies and main elements of the two models used by Modus: the Mercury passenger mobility model and the EUROCONTROL R-NEST tool. These models will be run separately, with results reported in D5.2 (Final Project Results Report). However, the (new) underpinning commonalities to support the inclusion of a rail layer in both models, and for each to model the full door-to-door context of passenger multimodal journeys, have been presented herein. This has included the formulation of city archetypes (a combination of air and rail transport mobility by NUTS3 regions) and passenger archetypes (based on socio-economic characterisations) to render the models tractable.

Some of the parameter values presented may be revised during model calibration, e.g. in order to ensure sensible model outputs and appropriate differentiation between the scenarios, in both models. Once the final parameterisations of the Mercury and R-NEST models are concluded, a comparison table between the two will be presented in D5.2, to support the interpretation of the corresponding results. To the greatest extent possible, the two sets of model scenarios have been aligned, not least through basically common assumptions (e.g. relating to flight bans) and the addition to each of common rail layers, although each model faces particular constraints (e.g. the absence of full D2D passenger itineraries in R-NEST and of higher resolution airspace structures in Mercury), and some differences in air traffic growth assumptions pertain. Furthermore, disruption is not applied to the R-NEST model (except through typical ATFM delays).

EUROPEAN PARTNERSHIP

Co-funded by
the European Union

7 References

[1] Modus Grant Agreement Description of Action - GA-891166-Modus

[2] Behrens, C. and Pels, E., Intermodal competition in the London–Paris passenger market: High-Speed Rail and air transport, Journal of Urban Economics, Volume 71, 2021, https://doi.org/10.1016/j.jue.2011.12.005.

[3] P. Arich, T. Bolic, I. Laplace, N. Lenoir, S. Parenty, A. Paul, and C. Roucolle, Substitution path between air and rail in Europe: a measure of demand drivers, Air Transport Research Society World Conference, 2022.

[4] Delgado, L., Gurtner, G., Mazzarisi, P., Zaoli, S., Valput, D., Cook, A. and Lillo, F., Network-wide assessment of ATM mechanisms using an agent-based model, Journal of Air Transport Management, Volume 95, 2021, https://doi.org/10.1016/j.jairtraman.2021.102108.

[5] UIC (International Union of Railways), Multiple East-West Railways Integrated Timetable Storage (MERITS) database, https://uic.org/passenger/passenger-services-group/merits.

[6] DATASET2050 project, https://dataset2050.eu/.

[7] DATASET2050 project, D2.2 Data Driven Model, 2016.

[8] DATASET2050 project, D4.2 Future Supply Profile, 2017.

[9] DATASET2050 project, D5.2 Assessment Execution, 2017.

[10] Modus project, D3.2 Demand and supply scenario and performance indicators, 2021, https://modus-project.eu/wp-content/uploads/2021/12/Modus_891166_D3.2_Scenarios-and-indicators_V1.1.pdf.

[11] Wikipedia, Truncated normal distribution, https://en.wikipedia.org/wiki/Truncated_normal_distribution.

[12] Gurtner, G., Delgado, L. and Valput, D., An agent-based model for air transportation to capture network effects in assessing delay management mechanisms, Transportation Research Part C: Emerging Technologies, Volume 133, 2021, https://doi.org/10.1016/j.trc.2021.103358.

[13] EUROCONTROL, European Aviation in 2040 - Challenges of Growth, 2018.

[14] Vista project, https://vista-eu.com/.

[15] EUROCONTROL, Aviation Outlook 2050, April 2022.

[16] BEACON project, D3.2 Industry briefing on updates to the European cost of delay, 2021, https://www.beacon-sesar.eu/wp-content/uploads/2022/10/893100-BEACON-D3.2-Industry-briefing-on-updates-to-the-European-cost-of-delay-V.01.01.00-1.pdf

[17] SESAR JU, European ATM Master Plan: Edition 2020, 2019, https://www.atmmasterplan.eu/.

[18] United Nations, World Urbanization Prospects: The 2018 Revision, 2019, https://population.un.org/wup/Publications/.

[19] IATA, Net-Zero Carbon Emissions by 2050, 2021, https://www.iata.org/en/pressroom/2021-releases/2021-10-04-03/.

[20] EUROCONTROL, Aviation Sustainability Briefing, 2021, https://www.eurocontrol.int/sites/default/files/2021-12/eurocontrol-aviation-sustainability-briefing-edition-5.pdf.

[21] European Commission, Sustainable and smart mobility strategy: putting European transport on track for the future, 2020.

[22] EUROCONTROL, All-Causes Delay to Air Transport in Europe, August 2019.

[23] EUROCONTROL, All-Causes Delay to Air Transport in Europe, September 2019.

[24] European Environmental Agency, Decarbonising road transport — the role of vehicles, fuels and transport demand, EEA report no 2/2022, 2022.

[25] UIC (International Union of Railways) and Community of European Railway and Infrastructure Companies, Rail transport and environment: facts and figures, 2015.

[26] Performance Review Commission, Performance Review Report - an assessment of air traffic management in Europe during the calendar Year 2019, 2020

EUROPEAN PARTNERSHIP

8 Acronyms

AAGR	average annual growth rate
ACC	area control centre
ATFCM	air traffic flow capacity management
ATM	air traffic management
BADA	base of aircraft data
CASA	Computer Assisted Slot Allocation
CODA	EUROCONTROL Central Office for Delay Analysis
D2K	door-to-kerb
D2P	door-to-platform
D2S	door-to-station
ECAC	European Civil Aviation Conference
FIPS	flight increase process
G2G	gate-to-gate
G2K	gate-to-kerb
GDP	gross domestic product
GEOSTAT	GEOSTAT is a section of Eurostat dedicated to geospatial statistics
HSR	high-speed rail
ID	identification
K2D	kerb-to-door
K2G	kerb-to-gate
NUTS	nomenclature of territorial units for statistics
OD	origin-destination
P2D	platform-to-door
P2P	platform-to-platform
R-NEST	EUROCONTROL Research Network Strategic tool
S2D	station-to-door

EUROPEAN PARTNERSHIP

Co-funded by
the European Union

S2T   station-to-train

T2S   train-to-station

EUROPEAN PARTNERSHIP

Appendix A   Current and planned HSR in Europe

Table 16: Current and planned HSR in Europe

Routes with HSR service existing/planned	Country	Year
Linz - Wels	Austria	1990
St. Pölten - Ybbs		2001
Amstetten - St. Valentin		2003
St. Valentin - Asten-St. Florian		2007
Vienna Knot Hadersdorf - St. Pölten		2012
Radfeld Knot - Baumkirchen Knot		2012
Wels - Attnang-Puchheim		2012
Ybbs - Amstetten		2016
Vienna Stadlau - Slovakian border		2022
Vienna Inzersdorf Ort - Wr. Neustadt		2023
Graz - Klagenfurt		2025
Border Gloggnitz - Mürzzuschlag		2026
Volders-Baumkirchen - Italian border		2027
Linz - Wels		2026
Gänserndorf - Czech border		2028
Mattstetten - Rothrist	Switzerland	2004
Solothurn - Wanzwil		2004
Frutigen - Visp (Lötschberg base tunnel)		2007
Erstfeld - Biasca (Gotthard base tunnel)		2016
Giubiasco/S. Antonino - Vezia (Ceneri base tunnel)		2020
Brussels - French border	Belgium	1997
Leuven - Liège		2002
Liège - German border		2009

EUROPEAN PARTNERSHIP

Routes with HSR service existing/planned	Country	Year
Antwerp - Dutch border		2009
Hoofddorp - Rotterdam West	Netherlands	2006
Rotterdam Lombardijen - Belgian border		2006
Plzeň - Domažlice - German border	Czech Republic	2027
Prague - Brno		2028
Prague - Hradec Králové		2028
Šakvice – Břeclav (A / SK border)		2028
Přerov - Ostrava		2029
Modřice - Šakvice		2029
Brno - Přerov		2030
Prague - Litoměřice		2030
Poříčany - Světlá nad Sázavou		2031
Velká Bíteš - Brno		2031
Světlá nad Sázavou - Velká Bíteš		2034
Poříčany - Hradec Králové		2040
Odb. Veltrusy - Most		2040
Copenhagen - Ringsted	Denmark	2019
Tallinn - Latvian border	Estonia	2026
Helsinki - Turku	Finland	1995
Helsinki - Oulu		2001
Jämsänkoski - Jyväskylä		2001
Kinni - Otava		2006
Kerava - Lahti		2006
Lahti - Luumäki		2009
Estonian border - Lithuanian border	Latvia	2026
Latvian border - Polish Border	Lithuania	2026

EUROPEAN PARTNERSHIP

Routes with HSR service existing/planned	Country	Year
Kaunas - Vilnius		2026
Stockholm - Örebro	Sweden	1991
Gothenburg - Lund		2008
Nyland - Umeå		2009
Sundsvall - Nyland		2010
Gothenburg - Kornsjø		2012
Umeå - Dåvå		2024
Lund - Arlöv		2024
Varberg - Hamra (Varbergtunnel)		2025
Ängelholm - Maria		2025
Järna - Linköping		2025
Dingersjö - Sundsvall		2028
Myrbacken - Uppsala		2029
Gävle - Kringlan		2032
Dåvå - Skellefteå		2033
Gothenburg - Borås		2035
Hässleholm - Lund		2035
Maria - Helsingborg		2035
LGV Paris Sud-Est	France	1981/1983
LGV Atlantique		1989/1990
LGV Rhône - Alpes (rail bypass of Lyon)		1992/1994
LGV Nord (inc. London - Brussels link		1994/1996
LGV Interconnexion Est IDF		1994/1996
LGV Méditerranée		2001
LGV Est Europe (first phase)		2007
Perpignan - Spanish border		2010

EUROPEAN PARTNERSHIP

Routes with HSR service existing/planned	Country	Year
LGV Rhin-Rhône Branche Est (first phase)		2011
LGV Est Europe (second phase)		2016
LGV Bretagne Pays de la Loire (BPL)		2017
LGV Tours - Bordeaux (SEA)		2017
Modernisation of HSL Paris-Lyon and Lyon bypass		2025
Wendlingen - Ulm	Germany	2022
Stuttgart - Wendlingen		2024
Karlsruhe - Rastatt - (Basel)		2024
Buggingen - Katzenbergtunnel - (Basel)		2025
(Karlsruhe) - Katzenberg tunnel - Basel		2025
(Karlsruhe) Riegel - Buggingen (Basel)		2031
(Karlsruhe) - Offenburg - Riegel - (Basel)		2035
Belgrade - Niš	Serbia	2023
Rome - Florence (first section)	Italy	1977
Rome - Florence (second section)		1985
Rome - Florence (third section)		1986
Rome - Florence (fourth section)		1992
Turin - Novara		2006
Padova - Venice		2007
Milan - Bologna		2008
Naples - Salerno		2008
Rome - Naples		2009
Novara - Milan		2009
Florence - Bologna		2009
Milan (Treviglio) - Brescia		2016
Genoa - Milan (Tortona)		2022

Routes with HSR service existing/planned	Country	Year
Grodzisk Mazowiecki - Zawiercie	Poland	2015
Warsaw - Poznan / Wroclaw		2030
Warsaw - Bialystok - Eák		2030
Elk - Lithuanian border (Rail Baltica)		2030
Knapówka - Katowice / Kraków		>2030
Wroclaw - Czech border		>2030
Poznan - German border		>2030
Katowice - Czech border		>2030
Warsaw - Toruń - Gdańsk		>2030
Évora - Caia	Portugal	2023
Madrid - Sevill	Spain	1992
Madrid - Lleida		2003
Zaragoza - Huesca		2003
(Madrid -) La Sagra - Toledo		2005
Córdoba - Antequera-Santa Ana		2006
Lleida - Camp de Tarragona		2007
Madrid - Segovia - Olmedo - Valladolid		2007
Antequera-Santa Ana - Málaga		2007
Antequera-Santa Ana - Málaga		2008
Bypass Madrid		2009
Santiago - A Coruña		2009
(Madrid -) Torrejón de Velasco - Valencia		2010
Albacete Junction - Albacete		2010
Figueres - French border (- Perpignan)		2010
Ourense - Santiago		2011
Bypass Yeles		2012

EUROPEAN PARTNERSHIP

Co-funded by
the European Union

Routes with HSR service existing/planned	Country	Year
Barcelona - Figueres		2013
Albacete - Alicante/Alacant		2013
Santiago - Vigo		2015
Sevilla - Cádiz		2015
Valladolid - León		2015
Olmedo - Zamora		2015
Valencia - Vandellós		2019
Antequera-Santa Ana - Granada		2019
Vandellós - Tarragona		2020
Zamora - Pedralba		2020
Murcia Junction - Orihuela - Beniel		2021
Pedralba - Ourense		2021
Beniel - Murcia		2022
Venta de Baños - Burgos		2022
León - Pola de Lena (Pajares New pass)		2022
Vitoria Gasteiz - Bilbao / San Sebastián		2028
Fawkham Junction - Channel Tunnel	United Kingdom	2003
London - Southfleet Junction		2007
London - Birmingham		2026
Birmingham - Crewe		2028
Crewe - Manchester/Wigan		2035
Birmingham - Leeds/York		2035